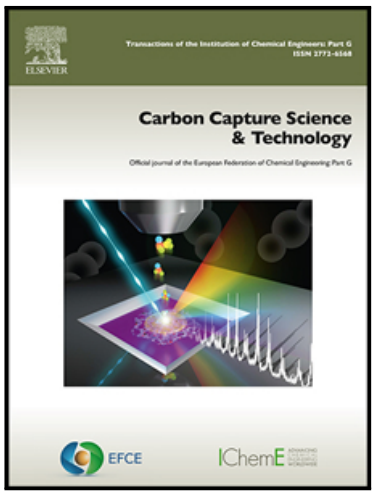

Optimisation of Reaction Temperature during Carboxylation of Single and Mixed Model Bio-derived Phenolics as Effective Route for CO_2 Utilisation

Omar Mohammad , Jude A. Onwudili , Qingchun Yuan , Robert Evans

PII: S2772-6568(25)00081-8
DOI: https://doi.org/10.1016/j.ccst.2025.100442
Reference: CCST 100442

To appear in: *Carbon Capture Science & Technology*

Received date: 27 March 2025
Revised date: 12 May 2025
Accepted date: 13 May 2025

Please cite this article as: Omar Mohammad , Jude A. Onwudili , Qingchun Yuan , Robert Evans , Optimisation of Reaction Temperature during Carboxylation of Single and Mixed Model Bio-derived Phenolics as Effective Route for CO_2 Utilisation, *Carbon Capture Science & Technology* (2025), doi: https://doi.org/10.1016/j.ccst.2025.100442

Highlights

- Investigation of Kolbe-Schmitt reactions of single and mixtures of phenolic sodium salts
- Influence of reaction temperature on carboxylation products studied from 175 – 225 °C
- Mono-carboxylation was favoured across all temperatures with the individual phenolics
- Competing CO_2 insertion at ortho and para positions in mono-carboxylated products observed
- With mixed phenolic sodium salts, formation of valuable dicarboxylic acids favoured at 225 °C

Optimisation of Reaction Temperature during Carboxylation of Single and Mixed Model Bio-derived Phenolics as Effective Route for CO_2 Utilisation

Omar Mohammad[a], Jude A. Onwudili*[a,b], Qingchun Yuan,[a,b], Robert Evans,[b]

[a] O. Mohammad, J.A. Onwudili, Q. Yuan. Energy and Bioproducts Research Institute, Aston University, Aston Triangle, Birmingham, B4 7ET, West Midlands, United Kingdom

[b] J.A. Onwudili, Q. Yuan, R. Evans, Department of Chemical Engineering and Applied Chemistry, Aston University, Aston Triangle, Birmingham, B4 7ET, West Midlands, United Kingdom

*Corresponding Author's E-mail: j.onwudili@aston.ac.uk

Abstract

This study investigates the temperature-dependent carboxylation of single and mixed biomass-derived phenolic sodium salts with CO_2 via the Kolbe–Schmitt reaction. Reactions were performed at T = 175–225 °C, t = 2 h, and pCO_2 = 30 bar. Five model phenolics; phenol, 2-cresol, guaiacol, catechol, and syringol were examined individually and in mixtures. Characterisation via high-performance liquid chromatography (HPLC) and nuclear magnetic resonance (NMR) analysis showed that 2-hydroxybenzoic and dicarboxylic acids were favoured at higher temperatures, while 4-hydroxybenzoic acids dominated at 175 °C. In mixtures, dicarboxylic acid yields increased significantly, reaching 41.9% for 2,3-dihydroxyterephthalic acid and 20.5% for 2-hydroxyisophthalic acid. These dicarboxylic acids possess up to 10-fold higher market value than their monocarboxylic counterparts. Syringic acid synthesis via Kolbe–Schmitt is reported here for the first time, with yields rising to 33.0% in mixtures versus <2.0% molar yield when reacted individually. The study also presents the first detailed mechanistic explanation of Brønsted acid–base interactions and temperature-driven selectivity in phenolic salt carboxylation. While previous research suggested that producing phenolics solely from lignin was not viable, this work demonstrates that CO_2 incorporation not only enhances product value but also narrows product distribution and enables broader industrial applicability - ultimately opening new opportunities for potential large-scale, economically viable CO_2 utilisation.

Keywords: CO_2 utilisation, high-value organic chemicals, hydroxybenzoic acids, dicarboxylic acids, model biomass-derived phenolics, chemical fixation and reaction mechanisms

1 Introduction

The concept of deep decarbonisation represents an ambitious goal of replacing the global carbon-intensive chemical and energy industries with renewable low-carbon alternatives, with the aim of limiting global temperatures to below 2 °C. However, this concept is either unachievable or significantly expensive without carbon capture, utilisation, and storage (CCUS) technologies [1]. Coupling CCUS with CO_2-based organic chemical production has the potential to deliver negative carbon emissions, which can support both environmental and economic objectives [2–4] of decarbonising the chemical and energy sectors.

Among emerging CCUS strategies, the Kolbe–Schmitt reaction represents a well-established method for incorporating molecular CO_2 into aromatic systems to produce hydroxybenzoic acids (HBAs), particularly salicylic acid [5,6]. While this reaction has traditionally employed fossil-derived phenolics, lignin-derived single-ring phenolic compounds (SPCs) such as phenol, catechol, guaiacol, cresol, and syringol present a sustainable alternative [7]. Lignin is a major component of lignocellulosic biomass and its generation is expected to reach 225 million tonnes per year by 2030 from biofuel production [8]. Despite this abundance, over 95% of lignin is burned for energy [9,10], with less than 5% used in value-added applications [11].

Converting lignin to SPCs can be achieved via various biochemical [12,13] and thermochemical routes [14–19]. The phenolic compounds can be reacted with CO_2 via Kolbe–Schmitt method to make high-value HBAs. Successful production of HBAs via this concept represents a sustainable value chain for lignin valorisation and CO_2 utilisation. HBAs are widely used in pharmaceuticals, cosmetics, food additives, polymers, and dyes [20–25]. For instance, the average market value of lignin-derived phenolics is around £211 per kilogram, whereas some HBA derivatives can go up to £5,500 per kilogram, a more than 25-fold increase in product value. Our conceptual approach depicted in **Fig 1.** is anticipated to provide triple benefits: (1) narrowing the product distribution for easier downstream separation, (2) increasing the market value of the output, and (3) contributing to CO_2 fixation as part of CCUS strategies.

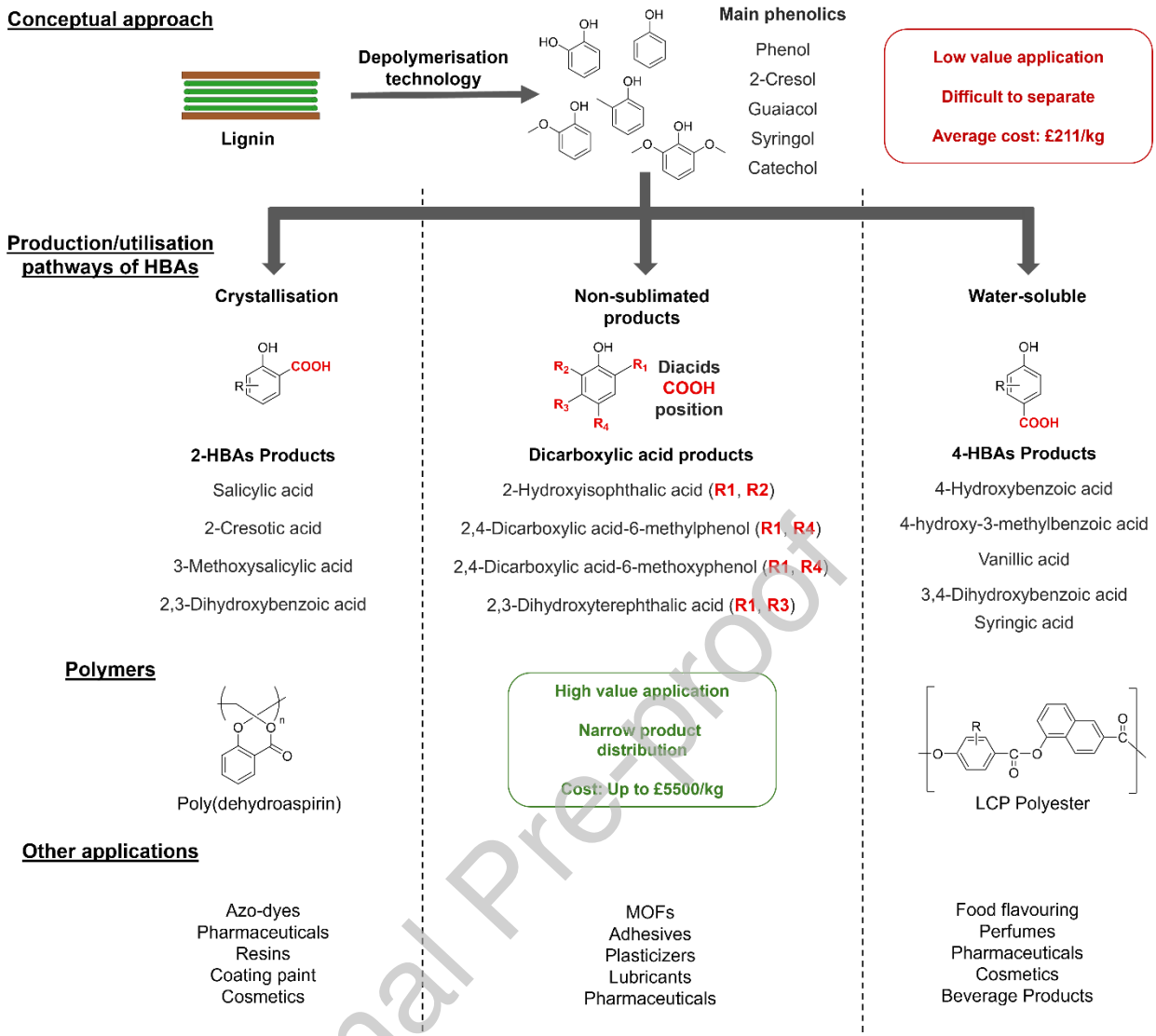

Fig 1. A conceptual approach to produce various hydroxybenzoic acids (HBAs) from biomass-derived phenolics, enabling their conversion into value-added HBAs for diverse applications, including the manufacturing of polymers, pharmaceuticals, cosmetics, food and flavouring agents, and metal-organic frameworks (MOFs).

While the Kolbe–Schmitt reaction is well understood for individual phenolics, temperature remains a key parameter that controls regioselectivity. Lower temperatures favour para-carboxylation, whereas higher temperatures increase ortho- and dicarboxylation [26–28]. These trends are only documented for some phenolics with no full product characterisation. Furthermore, no literature to date has explained how lignin-derived phenolics behave in mixtures under Kolbe–Schmitt conditions. In mixtures, substituent groups (e.g., methyl or methoxy) and relative acidity may influence the electronic distribution of the aromatic system, opening alternative carboxylation pathways involving Brønsted acid–base interactions and proton-sodium exchange [29].

Understanding such interactions is essential for designing selective and scalable carboxylation processes based on realistic biomass feedstocks.

This study presents, for the first time, a systematic investigation of product distribution both individual and mixed lignin-derived phenolics under gas-solid Kolbe-Schmitt reaction. Five model compounds - phenol, 2-cresol, guaiacol, catechol, and syringol - were converted into their sodium salts and reacted with CO_2 at 30 bar across three temperatures (175 °C, 200 °C, and 225 °C) for 2 hours. High-performance liquid chromatography (HPLC) and nuclear magnetic resonance (NMR) spectroscopy were used to characterise product distributions and yields. The findings provide novel insights into the temperature-dependent selectivity and interactions between phenolics in mixtures, information not previously reported and offer a practical basis for the development of CCU integrated lignin valorisation platforms.

2 Materials and Methods

2.1 Materials

The phenolic precursor compounds used in this study for the preparation of their respective sodium salts included phenol (>99% purity), 2-cresol (99% purity), guaiacol (>99% purity), catechol (>99% purity), and syringol (99% purity). These phenolics were also formed as reaction products and were incorporated into the external calibration data. The corresponding hydroxybenzoic acid products of these phenolics were purchased for quantification using the external standard method. These included salicylic acid (>99% purity), 4-hydroxybenzoic acid (>99% purity), 2-cresotic acid (99% purity), 4-hydroxy-3-methylbenzoic acid (97% purity, Sigma Aldrich), 3-methoxysalicylic acid (97% purity), vanillic acid (98% purity), 2,3-dihydroxybenzoic acid (99% purity), 3,4-dihydroxybenzoic acid (97% purity), 2,3-dihydroxyterephthalic acid (97% purity, Sigma Aldrich), and syringic acid (97% purity). Sodium hydroxide (98.5% purity) was used for the formation of sodium salts of the phenolic compounds. Toluene (HPLC grade, 99.85% purity) was employed to wash the solid product post-reaction, while acetone (HPLC grade, 99.8% purity), formic acid (99% purity), methyl sulfoxide-d6 (NMR, 99.8% atom %D) and methanol (HPLC grade, 99% purity) were served as the solvent for sample work-up and analysis. All chemical reagents and solvents, unless specified otherwise, were obtained from Fisher Scientific (Leicester, UK). Carbon dioxide (industrial grade, 99.8% purity) was supplied in a 6.5 kg portable cylinder by BOC Gases, UK. Deionised water, used for sample preparation for HPLC analysis, was obtained in-house via a Q-pod system.

2.2 Preparation of phenolic salts and characterisation via back acidification methods

The sodium salt of phenolics (phenol, 2-cresol, guaiacol, syringol and catechol) were synthesised according to Kolbe's method. In the initial step, one mole of the phenolic compound was dissolved in an equimolar of sodium hydroxide solution (50 wt%). In case of catechol, one mole of catechol was dissolved into two moles of sodium hydroxide (50wt%) solution instead due to presence of two hydroxyl groups (-OH). The same method was carried for the preparation of the 5 phenolic compound mixture by reaction an equimolar of each of the phenol, and based on the total OH-groups, an equimolar amount of NaOH was added. The mixture was loaded in a glass liner of a 450 ml 4575A fixed head bench top Parr reactor vessel, equipped with a stirrer. All reactions used to produce the phenolic salts were performed at 130 °C for 4 h at a stirring rate 50 rpm. After the reaction, the reactor was cooled down to 40 °C (cooling below 40 °C caused solidification of the salts, presenting difficulty with recovery). The solution containing the phenolic salts was then transferred into a separate beaker. The beaker was left inside a vacuum oven at 40°C overnight to dry. The dry sodium salt of the phenolics were removed from the beaker, crushed to particle size of 125 - 250µm and stored in an air-tight container prior to use.

The purity of the synthesised sodium salts of the phenolic compounds was determined using the two-step back-acidification method developed in our recent work [30]. This method involves:

1) Gravimetric recovery of NaCl, with its measured mass compared against the theoretical value.
2) Quantifying the phenols formed after acidification using HPLC.

2.3 Carboxylation reaction

The conventional Kolbe-Schmitt reactions were conducted in a set of 4 × 10 mL Quadracell reactors previously described [30] supplied by Asynt (Isleham, Cambridgeshire, United Kingdom). In each reactor cell, a measured amount of phenolic salt (0.3 g) was added. All four reactor cells were then sealed onto the main reactor cap and purged with CO_2 to remove any residual air. The reactor system was pressurised to the target operating pressure (30 bar) using a two-stage piston cylinder regulator (GASARC, Tech Master GPT420 Series). The regulator valve controlled the maximum delivery pressure, and a digital pressure transducer monitored the pressure. The reactor was weighed before and after CO_2 pressurisation to determine the exact mass of CO_2 introduced.

The reactors were heated to the desired temperatures (225°C, 200°C, 175°C) at a rate of 10 °C/min. The reaction mixture was maintained at the target temperature for 2 hours before being

allowed to cool to room temperature. Reaction temperatures were controlled using an Asynt ADS-HP-NT magnetic stirrer hotplate, and pressure readings were displayed via a digital pressure gauge integrated with a cooling tower.

The overall methodology for the carboxylation of bio-derived phenolic salts is summarised in **Fig. 2**. In this present work, the methodology was refined to enhance the accuracy of HPLC analysis and mass balance calculations, involving the use of the carboxylated products in their salt form. In the refined procedure, a known mass of the carboxylated phenolic salt was transferred into a 10 mL volumetric flask, and a few drops of 12M HCl added along with a 50:50 v/v% acetone-water solution making total volume of 10 mL. This adjustment ensured that NaCl remains soluble in the solution, eliminating the need for separation, while also retaining the unreacted phenolics.

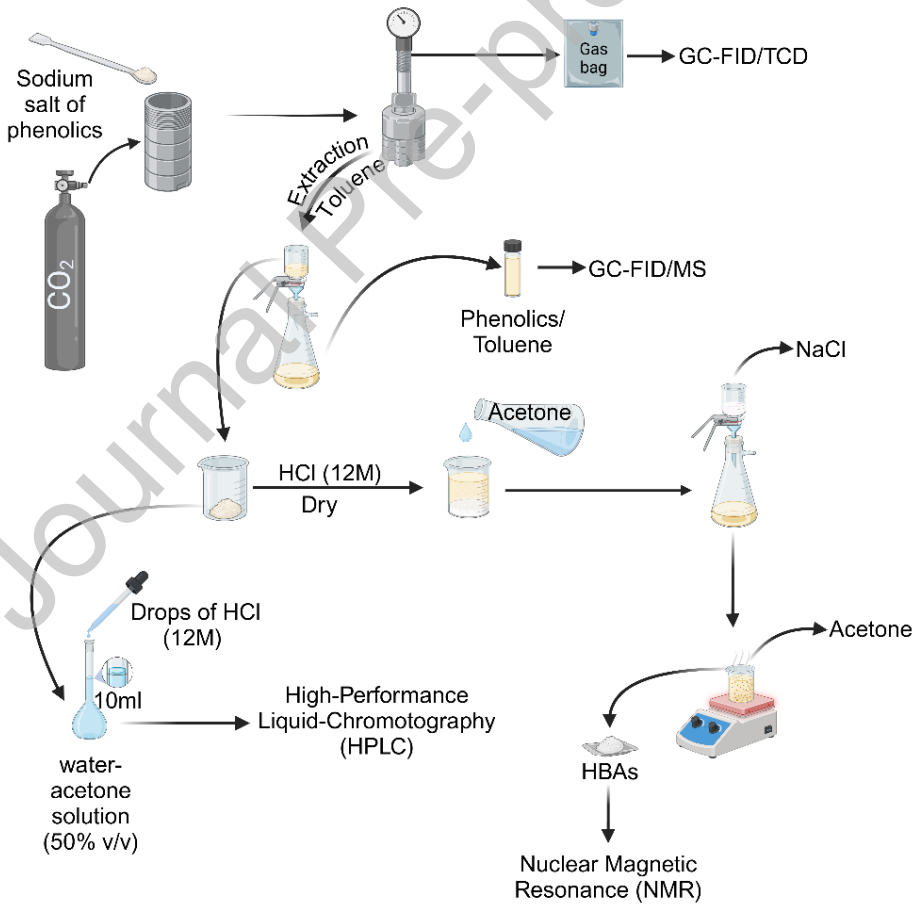

Fig 2. The overall methodology for carboxylation of sodium salt of various phenolics in this work "Created in BioRender. Mohammad, O. (2025) https://BioRender.com/s51k191" [31].

2.4 Characterisation of gases by Gas-Chromatography Flame Ionisation Detector and Thermal Conductivity Detector (TCD)

At the end of the reaction, after cooling the reactor, the gas phase was collected in the Tedlar bag and analysed using a Shimadzu GC-2014 gas chromatograph. The analytical conditions for this instrument have been previously reported by the research group [32]. Multiple analyses of the gas samples were performed, and the chromatograms indicated no or less than 1mol% of hydrocarbon gases.

2.5 Characterisation of phenolic compounds by Gas-Chromatography Flame Ionisation Detector and Mass Spectroscopy (GC-FID/MS)

After the reaction, a significant amount of phenolic compounds were detected in the conventional Kolbe-Schmitt reactions. The reactor and carboxylated products were washed with approximately 50 mL of toluene after the reaction to dissolve the phenolics formed during the reaction. A calibration curve for each of the phenolics (phenol, 2-cresol, guaiacol, catechol and syringol) were constructed, using an external standard method for quantification via GC-FID. GC-MS was employed as a qualitative method to detect any other potential toluene-soluble organics. The results confirmed that phenolics were the main toluene-soluble organics (see Supplementary Information **Figure S1**). Full details of the calibration method and the GC-FID/MS analysis are available in the recent publication [30].

2.6 Characterisation and quantification of Hydroxybenzoic acids (HBAs) by High-Performance Liquid-Chromatography (HPLC) and Nuclear Magnetic Resonance (NMR)

A high-performance liquid chromatography (HPLC) method was developed to effectively separate and quantify the products of the Kolbe–Schmitt reaction, as detailed in a recent study [30]. HBA products were identified by HPLC and quantified using calibration curves constructed from known masses of commercially available standards (see **Supplementary Figures S2–S6**). For unresolved peaks corresponding to dicarboxylic acids not available commercially, identification was performed

using ^{1}H NMR, focusing on the aromatic region (6–8.5 ppm), along with pulsed-field gradient NMR (PFG-NMR) and diffusion ordered spectroscopy (DOSY) to differentiate compounds based on their diffusion behaviour. These analyses were carried out on reaction products of 2-cresol, guaiacol, and catechol and the normalised concentrations of these dicarboxylic acids were quantified in mol%. For phenol-derived products, reference data can be found in [30,33]. Quantification of the identified dicarboxylic acids by HPLC was performed using 2,3-dihydroxyterephthalic acid as an external calibration standard, following a method previously validated against NMR measurements [30]. Additionally, calibration curves were generated for the unreacted phenolic precursors to determine their residual amounts for subsequent conversion calculations. All standards were prepared in a 50% v/v water-acetone solution, achieving calibration curves with R-squared values greater than 0.99 for all products and phenolic compounds. The HPLC analysis was conducted using a reverse-phase Kinetex 5 µm C18 100 Å column (250 × 4.6 mm, Phenomenex LTD, UK). The mobile phase consisted of water with 0.1% formic acid (Solvent A) and methanol (Solvent B) with the following gradient program: 5.0 min (90% A, 10% B), 20.0 min (70% A, 30% B), 30.0 min (50% A, 50% B), 40.0 min (30% A, 70% B), 45.0 min (10% A, 90% B), and 50.0 min (90% A, 10% B). The flow rate was set at 0.5 mL/min, with an injection volume of 10 µL. Detection was performed using a UV detector set at 254 nm with a 4 nm bandwidth, and the column temperature was maintained at 30°C. The quantified HBA products and their respective unreacted phenolic precursors are summarised in **Table 1.**

Table 1. Summary of phenolic salts and their corresponding hydroxybenzoic acids (HBAs). The carboxylation of phenolics were separated into three main categories, 2-HBA (main product), 4-HBAs (preferable at lower temperatures), and dicarboxylic acids (preferable at higher temperatures).

Phenolic compound	2-HBA	4-HBA	Dicarboxylic acid
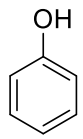	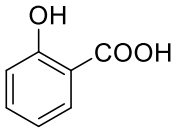	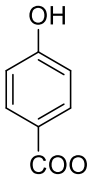	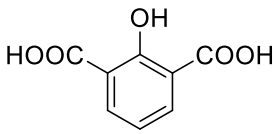
Phenol	Salicylic acid	4-Hydroxybenzoic acid	2-Hydroxyisophthalic acid *
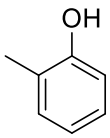	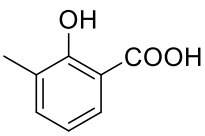	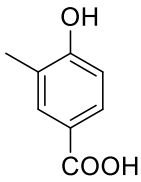	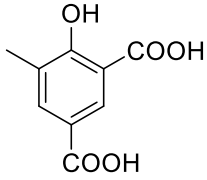
			*

2-cresol	2-Cresotic acid	4-hydroxy-3-methylbenzoic acid	2,4-dicarboxylic acid-6-methylphenol
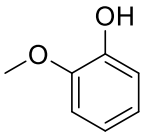	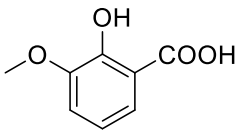	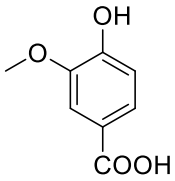	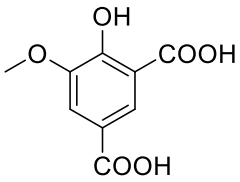
Guaiacol	3-Methoxysalicylic acid	Vanillic acid	2,4-dicarboxylic acid-6-methoxyphenol
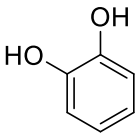	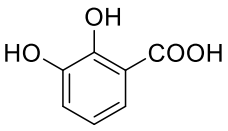	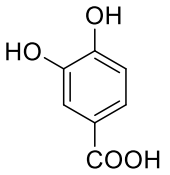	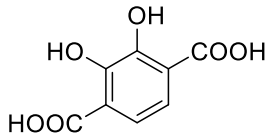
Catechol	2,3-Dihydroxybenzoic acid	3,4-Dihydroxybenzoic acid	2,3-Dihydroxyterephthalic acid
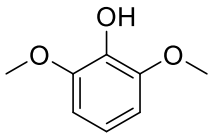	**N/A**	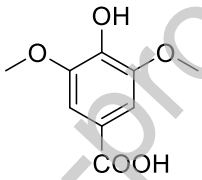	**N/A**
Syringol		Syringic acid	

Note: Calibration curves were constructed with commercially available HBAs as external standards. Dicarboxylic acid compounds marked with an asterisk (*) were identified using NMR, as they were not commercially available and quantified using 2,3-dihydroteretphalic acid as an external standard instead.

2.7 Characterisation by Nuclear Magnetic Resonance (NMR) Spectroscopy: Correlation Spectroscopy (COSY) and Diffusion-Ordered Spectroscopy (DOSY) Analyses

NMR measurements were conducted to identify unresolved peaks observed in the HPLC chromatograms, corresponding to dicarboxylic acid products. All NMR measurements were carried out on non-spinning on a 500 MHz Bruker Advance NEO spectrometer, using a 5 mm iProbe equipped with a z-gradient coil producing a maximum gradient of 50.5 G cm^{-1}. Each NMR sample contained *ca*. 0.01 g of the HBA products acquired at 225°C, with TMS as a reference, in 1 mL DMSO-d_6 solution. All NMR measurements were performed at 298.15 K. Correlation spectroscopy (COSY) experiments used a gradient-enhanced double-quantum-filtered sequence. 128 increments, each consisting of 16 transients of 2048 data points, were acquired, for a total experiment time of *ca*. 0.5 hours. Diffusion NMR experiments used a Oneshot sequence [34]. The use of viscous DMSO-d_6 as a solvent removed any possible effects of convection from the measurements in bulk solution [35]. Ten magnetic field gradient amplitudes, from 6.4 to 25.7 G cm^{-1}, were used and

incremented in equal steps of gradient squared. The gradient encoding time for all experiments was 1 ms and all gradients were half-sine in shape. The diffusion delay time, Δ, was set according to the species studied, to obtain ca. 80% attenuation of signals. For each gradient amplitude, 64 transients of 16384 complex data points were acquired for a total experimental time of *ca*. 1 hr. DOSY spectra and associated diffusion coefficients were subsequently produced using the DOSY Toolbox software package [36]

2.8 New Approach for Accurate Yield and Conversion Determination by Separating Free Phenols in the Kolbe–Schmitt Reaction

The molar yield for each product was calculated relative to the initial moles of its corresponding sodium salt of the phenolic compound, as defined by the stoichiometric reaction in Scheme 1 using *Equation 1*.

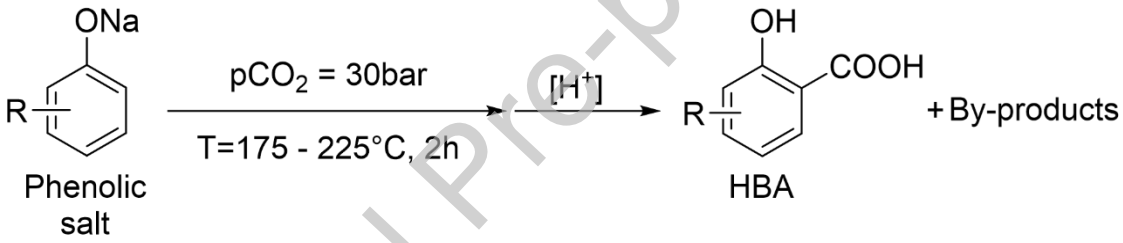

Scheme 1. Simplified stoichiometric reaction equation for conventional Kolbe-Schmitt reaction.

$$\text{Molar yield } (\%) = \frac{nProduct}{nPHX_{fed}} \times 100 \quad (1)$$

Here, the moles of products ($nProduct$) include 2-HBAs, 4-HBAs, dicarboxylic acids which were quantified using HPLC, as well as phenolic compounds quantified by GC-FID/MS; all formed during the reaction (see **Fig. 2**). $nPHX_{fed}$ is the moles of the phenolic salt initially fed to the reactor.

The conversion was calculated as the ratio of unreacted moles of sodium salt of phenolics ($nPh_{unreacted}$) to the initial moles ($nPHX_{fed}$), expressed as a percentage as shown in *Equation 2*.

$$Conversion\ (\%) = 1 - \left(\frac{nPh_{unreacted}}{nPHX_{fed}}\right) \times 100 \approx \frac{\sum_n products}{nPHX_{fed}} \times 100 \quad (2)$$

Finally, validation of this method was conducted through ensuring the sum moles for all products ($\sum_n products$) and unreacted sodium phenolic salt ($nPH_{unreacted}$) accounts for the initial amount of phenolic salt fed to the reactor ($nPHX_{fed}$). An example is shown in *Equation 3.*

$$n2HBA + n4HBA + nDicarboxylic\ acid + nPh_{toluene} + nPh_{unreacted} \leq nPHX_{fed} \quad (3)$$

The carboxylation products of each phenolic salt are summarised in **Table 1**. A mass balance exceeding 95% was achieved in all cases. A key distinction of this study compared to previous works is the development of a methodology to separate the free phenol formed during the reaction from the carboxylated products [30]. Typically, reaction products are quenched with water, leaving the free phenol in the aqueous phase along with water-soluble products. Upon acidification and characterisation, this free phenol is often assumed to be unconverted PhONa [6,37–39]. In contrast, our approach involved first extracting the free phenols formed during the reaction using toluene, allowing for a more accurate determination of conversion. This method confirms that the free phenols originate from the reaction itself and should be considered as products rather than unreacted starting material as demonstrated in a recent work [30].

3 Results and Discussion

3.1 Mechanistic insights and temperature-dependent reactivity of phenol in the Kolbe-Schmitt reaction

In the Kolbe-Schmitt reaction, the formation of sodium phenoxides in the first step is crucial as it initiates the resonance effect in phenolics, enhancing the nucleophilicity of the phenoxide ions. To ensure optimal reactivity, it is essential to start with a highly pure phenoxide ion with minimised moisture content. Based on the percentage of recovered phenol and the NaCl content after acidification, above 95% purity of the prepared salts were achieved (see **Supplementary Materials, Table S1**). The resonance structures of the phenoxide ion reveal that the negative charge is delocalised primarily at positions **2**, **4**, and **6** (with positions **2** and **6** being ortho isomers) (**Scheme 2**) [40]. This delocalisation creates electron-rich sites at these positions, enabling the electrophilic CO_2 to preferentially react with the nucleophilic phenoxide ion [7].

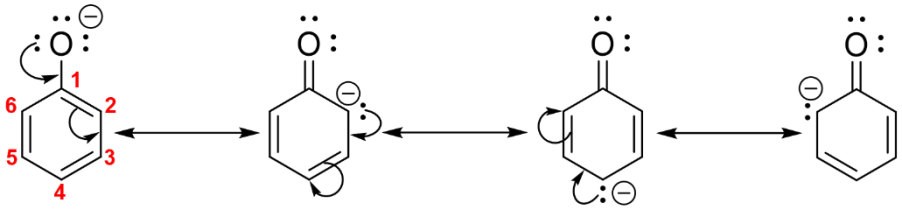

Scheme 2: Delocalisation of the alkoxide ion across the benzene ring, illustrating resonance effects that occur exclusively at positions **2**, **4**, and **6**.

This increased nucleophilicity facilitates the generation of disodium salicylate upon reaction with CO_2 at either the **2**- or **4**-position [30]. However, the reaction predominantly favours the 2-hydroxybenzoic acid (2-HBA) pathway, and this preference can be attributed to several factors. Firstly, as with phenol, there are two possible ortho positions (**2** and **6**) and one para position (**4**) available for carboxylation. The ortho positions (**2** and **6**) are preferred due to their steric proximity to the hydroxyl group, which enhances electron density at these sites, making them more reactive toward CO_2. Additionally, the two ortho positions (**2** and **6**) provide a two-to-one positional advantage over position **4**, further increasing the likelihood of carboxylation at these sites. These positions also allow for better stabilisation of the intermediate and final product through favourable intramolecular interactions [30]. These factors collectively explain the predominant formation of 2-HBAs in the Kolbe-Schmitt reaction.

Scheme 3 illustrates the carboxylation pathway using phenol as a model compound. A new two-step reaction mechanism was proposed in recent work [30], which tracked reaction behaviour over a time range of 1 to 8 hours. In the first step, 2-disodium salicylate and phenol are formed. In the second step, 2-monosodium salicylate is generated as phenol reacts with 2-disodium salicylate, accompanied by the regeneration of sodium phenoxide. This mechanism was experimentally validated by introducing pure (free) phenol into the reaction of the conventional Kolbe-Schmitt reaction. The addition of phenol increased the yield of salicylic acid by 25.0% after 2 hours of reaction, compared to experiments without added phenol [30]. Building on this prior work, the present study not only investigates the effect of temperature but also applies the mechanistic insights gained from phenol as a model compound to other biomass-derived phenolics.

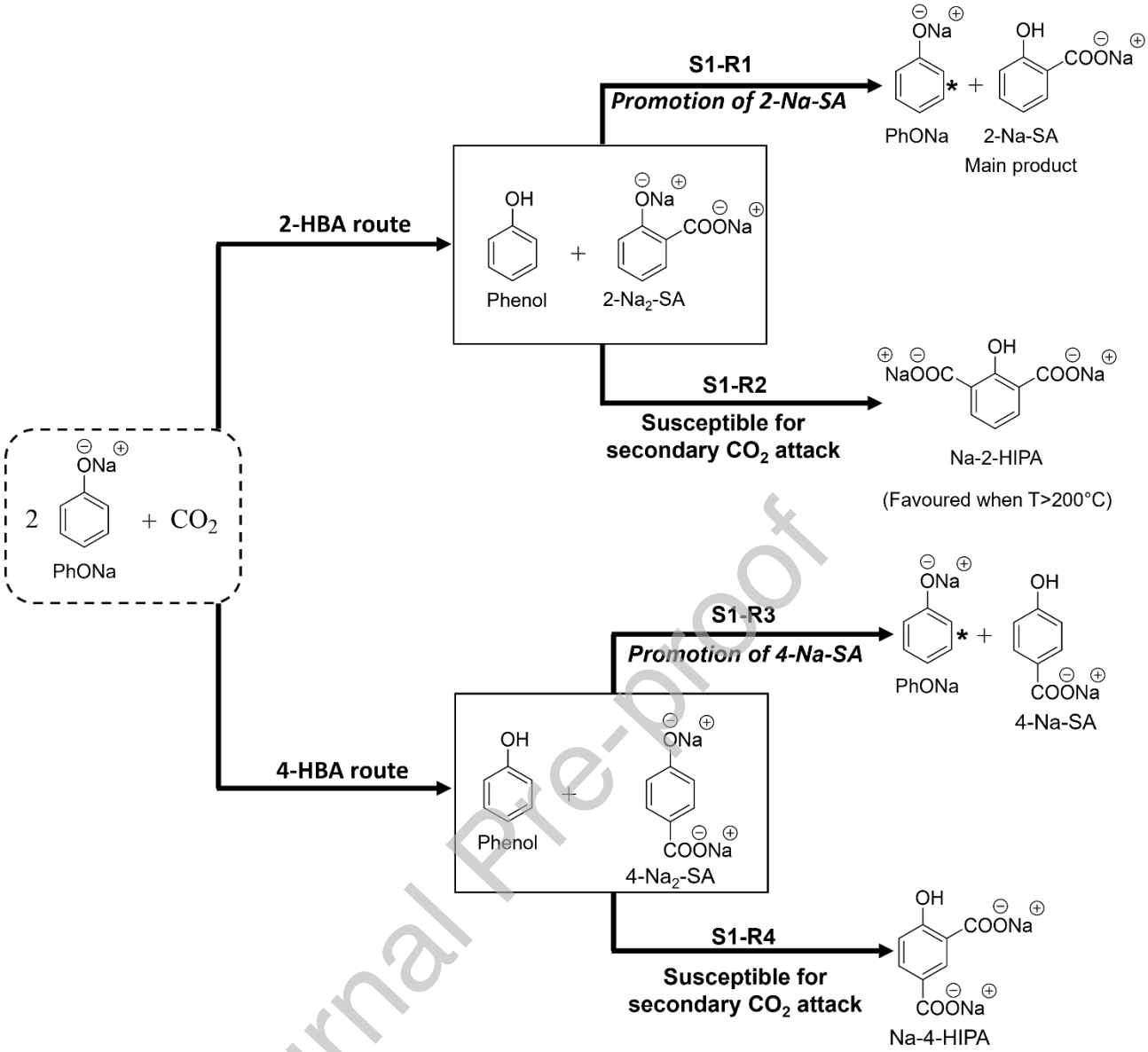

Scheme 3. Mechanistic pathways of phenol carboxylation. In the favourable 2-HBA route, the reaction begins with the formation of 2-disodium salicylate (2-Na_2-SA) and phenol, where phenol acts as a Brønsted acid. This leads to the formation of 2-Na-SA and sodium phenoxide (R1). The 2-Na-SA, being electron-rich, is susceptible to a second CO_2 attack at position 6, resulting in the formation of Na-HIPA (R2). In contrast, the less favourable 4-HBA route initiates with 4-Na_2-SA and phenol, generating 4-Na-SA and regenerating sodium phenoxide (R3). However, due to the instability of 4-Na_2-SA, this pathway is disfavoured, and progression to Na-HPA (R4) is unlikely. The regenerated sodium phenoxide (marked with *).

If the reaction takes the favourable route (**2-HBA route**), it proceeds with the *in-situ* formation of 2-monosodium salicylate (2-Na-SA) and sodium phenoxide (**S1-R1**), with phenol acting as a Brønsted

acid and 2-Na-SA as the Brønsted base. The regenerated sodium phenoxide (marked with *) undergoes successive reactions with CO_2, perpetuating the reaction cycle. However, the electronic configuration of 2-Na-SA, as indicated by Hammett's equation [41], makes it susceptible to another CO_2 attack at position 6, producing the sodium salt of 2-hydroxyisophthalic acid (Na-HIPA) ((**S1-R2**). Alternatively, the reaction may proceed through the less favourable **4-HBA route**, where the initial step produces phenol and 4-Na_2-SA. Similar to the 2-HBA pathway, phenol and 4-Na_2-SA can react to generate 4-monosodium salicylate (4-Na-SA) and regenerate sodium phenoxide ((**S1-R3**). However, due to the intrinsic instability of the **4-HBA route**, the formation of 4-Na_2-SA is already disfavoured, and its progression to form Na-HPA ((**S1-R4**) becomes even less likely [30].

Taking phenol as the first example, the carboxylation was carried out with CO_2 at a partial pressure of 30 bar for 2 hours across three temperatures: 175°C, 200°C, and 225°C. As observed in **Fig. 3**, the yield of salicylic acid was not significantly affected by temperature, with molar yields increasing slightly from 54.1% at 175°C to 55.6% at 200°C and 58.9% at 225°C. However, a more significant trend was noted for the molar yield of 4-hydroxybenzoic acid, which decreased as the temperature increased, with molar yields dropping from 9.75% at 175°C to 8.41% at 200°C and further to 5.42% at 225°C. These results align well with literature [6,26], which indicated that 4-hydroxybenzoic acid are favoured at lower temperatures and may be due to the reduced stability of 4-Na_2-SA at higher temperatures, thus shifting the reaction preference toward the **2-HBA route**.

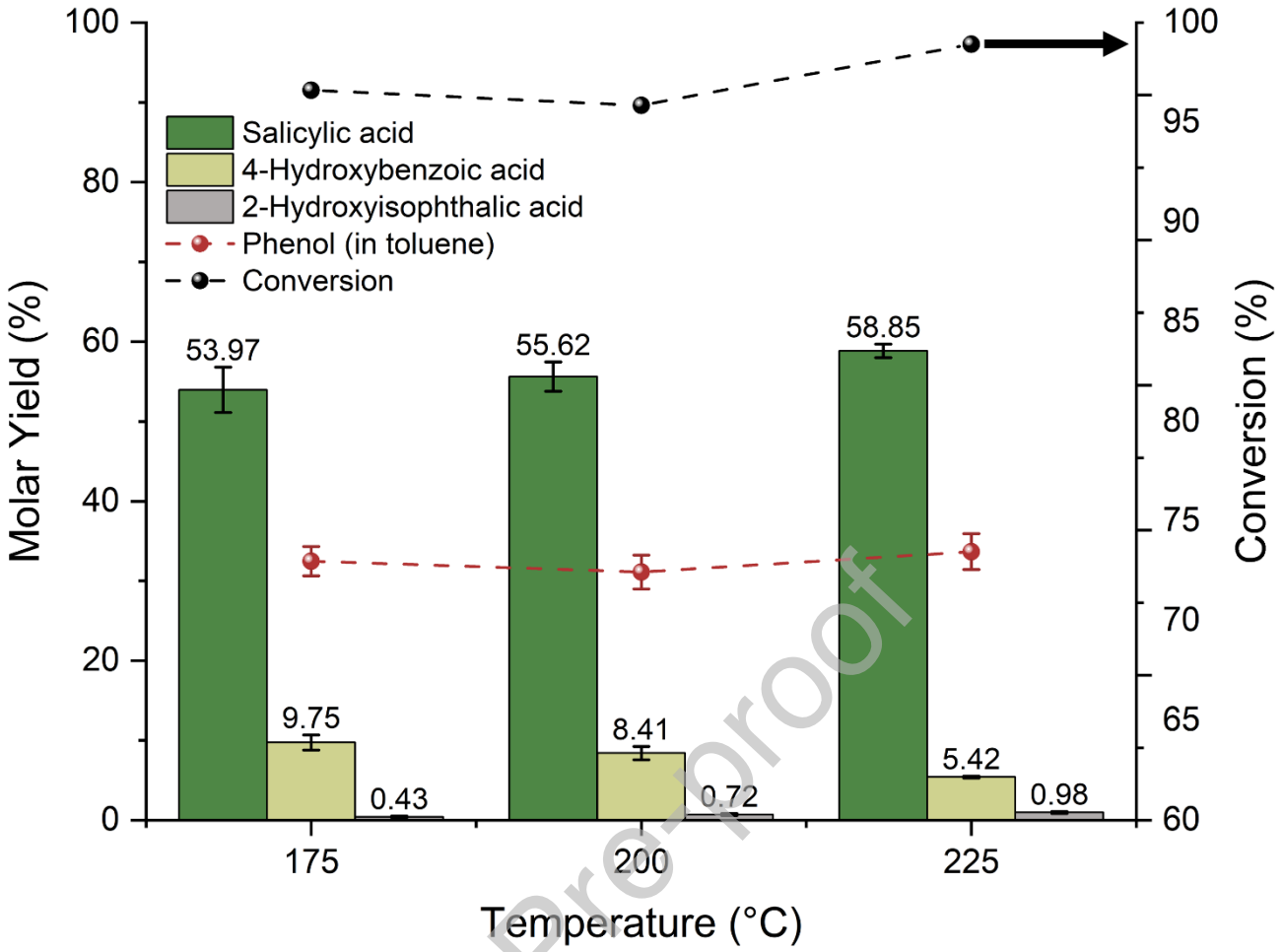

Fig. 3. Effect of temperature on product distribution and conversion of sodium phenoxide in the Kolbe-Schmitt reaction. Reaction conditions: t = 2 h, sodium phenoxide loading = 0.3 g, pCO_2 = 30 bar, and T = 175°C, 200°C, and 225°C. Error bars represent standard deviations.

The dicarboxylic acid, 2-hydroxyisophthalic acid, showed a steady increase in molar yields with temperature, from 0.43% at 175°C to 0.72% at 200°C and 0.98% at 225°C. These findings are consistent with previous reports and patents, which noted that terephthalic acid derivatives are favoured at temperatures above 200°C [26,28,30]. This trend suggests that **S1-R2** in **Scheme 3**, which involves a second carboxylation, requires higher energy to proceed. The reasoning lies in the reduced overall electron density of the aromatic ring caused by the presence of the electron-withdrawing carboxylate group (COO^-) [40]. The COO^- group deactivates the ring for further nucleophilic attack, however, at elevated temperatures, the energy barrier may be overcome, enabling the second carboxylation [30].

3.2 Temperature-dependent Reactivity of 2-Cresol in the Kolbe-Schmitt Reaction

Detailed carboxylation of 2-cresol or any cresols has not been previously reported. The available literature mainly compares the Kolbe–Schmitt and Marasse carboxylation methods for 2-cresol [42]. In this present study, the novel detailed characterisation of the carboxylation of 2-cresols has enabled better understanding of its reactivity and products formation. Using ^{1}H DOSY NMR, an unresolved peak observed in the HPLC spectrum (see **Figure S3**) was identified as 2,4-dicarboxy-6-methylphenol. However, due to the commercial unavailability of 2,4-dicarboxy-6-methylphenol, it was quantified using 2,3-dihydroxyterephthalic acid as a calibration standard, which agreed with the ^{1}H NMR quantification (**Figure S7 and S8**). The average deviation of just ±0.82 mol% was obtained between the two techniques (see **Table S2**), giving greater confidence of its accurate determination.

Experimental results presented in **Fig. 4** shows that the molar yield of 2-cresotic acid increased gradually between 175°C and 200°C, reaching 43.88% and 45.09%, respectively. However, further increasing the temperature to 225°C resulted in a drop in the yield to 40.94%. Although the conversion increased to 97.81% at 225°C, the higher conversion is likely due to thermal degradation of the carboxylated sodium salt of 2-cresol [43]. It is suggested that thermal degradation of the carboxylated products leads to increased formation of 2-cresol at elevated temperatures. Following these results, it would be recommended that carboxylation of 2-cresol to be conducted at lower temperatures, ideally at 200°C or slightly below.

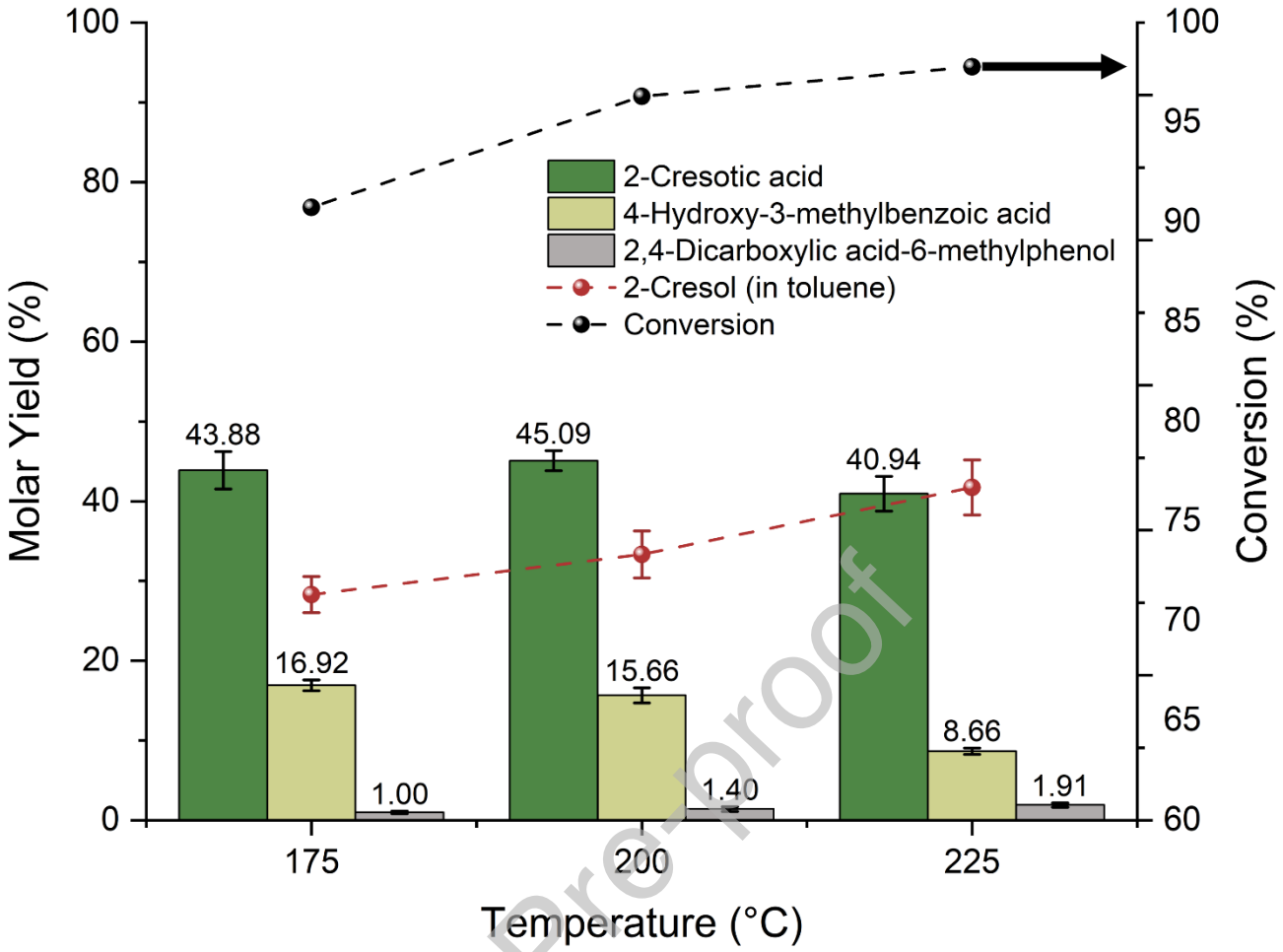

Fig. 4. Effect of temperature on product distribution and conversion of sodium 2-cresolate in the Kolbe-Schmitt reaction. Reaction conditions: t = 2 h, sodium 2-cresolate loading = 0.3 g, pCO_2 = 30 bar, and T = 175°C, 200°C, and 225°C. Error bars represent standard deviations.

The yields of 2-cresotic acid in this work (in just 2 hours) are similar or better to those previously reported in literature under different conditions of temperature and reaction times. For example, a study by Baine et al., [42] at 125°C for 8 hours under CO_2 pressure of 2000 psi (approximately 137.9 bar), yielded 44% of 2-cresotic acid using the Kolbe–Schmitt method [42]. Another study synthesised cresotic acids by carboxylation of cresols using sodium ethyl carbonate. The yield of 2-cresotic acid was reported as 38 wt% at 180°C after a reaction time of 8 hours under CO_2 pressure of 10 bar. However, no quantification of other products was performed, nor were details of product characterisation or reaction mechanisms provided [44]. Additionally, a high yield of 2-cresotic acid of 70% was reported on the basis of total hydroxy acids formed via the Marasse method employing potassium carbonate. Moreover, these studies did not quantify other potential products, such as carboxylation at position 4 (para) or formation of dicarboxylic acids.

A brief mechanism for the carboxylation of sodium 2-cresoloate is presented in **Scheme 4**. Similar to phenol, the main carboxylation route of 2-cresoloate is the **2-HBA route** in **Scheme 4**, forming compound **1b** and **1c** in the first step. Consequently, these compounds react with each other to form compound **1d**, while regenerating **1a**. Regarding carboxylation at position 4 (**1f**), the corresponding product, 4-hydroxy-3-methylbenzoic acid, followed a pattern similar to phenol products, with the highest yield observed at 175°C (16.92%) and decreasing with increasing temperature, yielding 15.66% at 200°C and 8.66% at 225°C. However, the higher yield at position 4 is also attributed to the structural nature of the cresol molecule, where the methyl group occupies one of the ortho positions, leaving only one ortho position (position 2) available for carboxylation. This creates greater competition between positions 2 and 4, unlike phenol, the symmetrical structure provided a two-to-one positional advantage for ortho (position 2 and 6) carboxylation over position 4. Therefore, 2-cresol has three possible reaction pathways, which influence its carboxylation behaviour (**Scheme 4**).

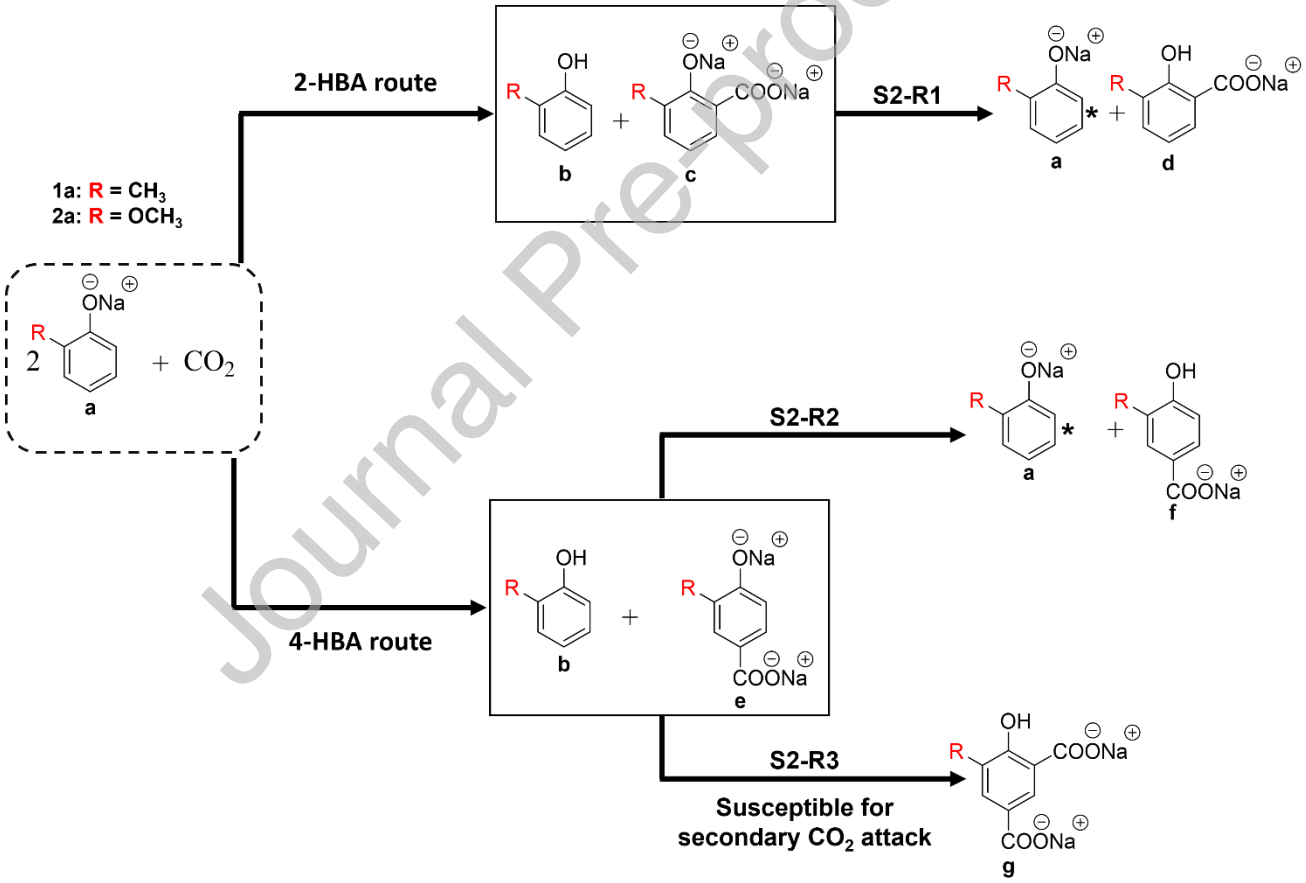

Scheme 4. Mechanistic pathways of carboxylation of sodium phenoxides with one ortho position substituted by an R group (R1 = CH_3, R2 = OCH3). The carboxylation proceeds via either the 2-HBA or 4-HBA route. In the 2-HBA route, intermediates **b** and **c** react further to form products **a** and

d. In the 4-HBA route, **b** and **e** can react to form **a** and **f**, or **e** can further react to form **g**. Sodium salts of phenolates, marked with an artistic (*), are regenerated during the reaction.

The dicarboxylic acid, 2,4-dicarboxylic acid-6-methylphenol forms via **S2-R3** to yield **1g**, showed an increase in molar yield with rising temperature, from 1.00% at 175°C to 1.40% at 200°C and 1.91% at 225°C. As illustrated in **Scheme 4**, the dicarboxylation at positions 2 and 4 is a direct consequence of the **4-HBA route**. The increased likelihood of the 4-HBA pathway promotes the formation of **1g**. However, the yield remains relatively low, as the second carboxylation step requires higher temperatures to overcome its energy barrier. This observation aligns with the general trend for dicarboxylation reactions, which demand elevated thermal energy for the second nucleophilic attack to proceed efficiently.

3.3 Temperature-dependent reactivity of guaiacol in the Kolbe-Schmitt reaction

The carboxylation of guaiacol has been scarcely studied in the literature. One available report describes the carboxylation of guaiacol via the Marasse method using anhydrous carbonates, yielding 47% at 175°C after 4 hours under a CO_2 pressure of 2000 psi (approximately 137.9 bar) [42]. However, the yield calculations were based solely on the hydroxybenzoic acid formed and did not account for the overall product yield. Additionally, no detailed product characterisation or elucidation of the reaction mechanism was presented. Similar to the cresol-derived products, an unresolved peak with a significant area percentage was observed in the HPLC analysis of guaiacol products. DOSY NMR revealed that this peak corresponded to a larger compound, which diffused more slowly. The compound was identified and quantified as 2,4-dicarboxy-6-methoxyphenol (see **Figure S7 and S9**), as described in Section 3.2, giving an average deviation of only ±0.80 mol% between ^{1}H NMR and HPLC measurements. (**Table S2**).

In this study a detailed accounting of the product distribution for the carboxylation of guaiacol has been carried out. As shown in **Fig. 5**, the main product is 3-methoxysalicylic acid, the yield increased with temperature, reaching 37.84% at 175°C, 45.03% at 200°C, and 52.53% at 225°C. This trend aligns with previous observations for phenol and 2-cresol, where the (2-HBA route) is favoured.

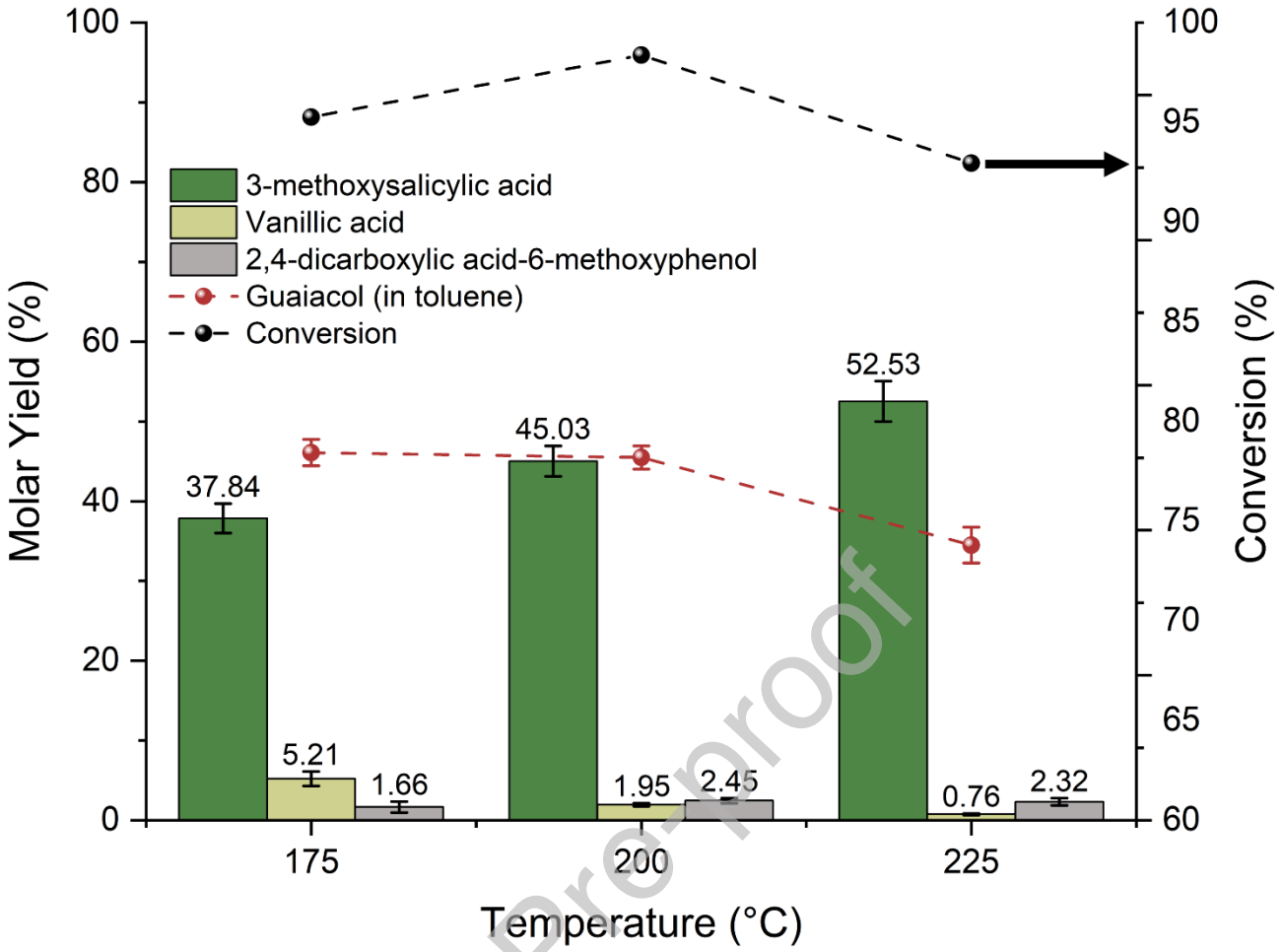

Fig. 5. Effect of temperature on product distribution and conversion of sodium guaiacolate in the Kolbe-Schmitt reaction. Reaction conditions: t = 2 h, sodium guaiacolate loading = 0.3 g, pCO_2 = 30 bar, and T = 175°C, 200°C, and 225°C. Error bars represent standard deviations.

Vanillic acid is produced through carboxylation at position 4. Consistent with the results in the previous section, its yield follows the 4-HBA route and is favoured at lower temperatures. The yield of **2f** (**Scheme 4**) decreased with increasing temperature, from 5.21% at 175°C to 1.95% at 200°C and 0.76% at 225°C. Notably, the yield of vanillic acid (position 4 carboxylation) is lower than that observed for phenol and 2-cresol. This can be attributed to the methoxy group at one of the ortho positions (2,6) on the aromatic ring. Acting as an electron-donating group, the methoxy group increases the electron density at position 2, making CO_2 more strongly attracted to this position and reducing the likelihood of carboxylation at position 4.

2,4-Dicarboxylic acid-6-methoxyphenol is the dicarboxylic product of guaiacol carboxylation. Its yield was 1.66% at 175°C, 2.45% at 200°C, and 2.32% at 225°C. The slight decrease observed at 225 °C compared to 200 °C falls within the experimental error margins; therefore, no definitive conclusion

can be drawn regarding a decrease in the formation of 2,4-dicarboxylic acid-6-methoxyphenol at higher temperatures. In general, this and previous studies indicate that higher temperatures favour the formation of dicarboxylated products [6,28]. Nevertheless, the formation of this particular product remains limited, likely due to its reliance on the less favourable 4-HBA pathway (via intermediate 2e). It is also noteworthy that the overall conversion slightly dropped between 200°C and 225°C, while the yield of 3-methoxysalicylic acid increased. This slight drop in conversion can be attributed to the formation of **2a** through **S2-R1** or **S2-R2**, where sodium guaiacolate (**2a**) is regenerated (see **Scheme 4**).

3.4 Temperature-dependent reactivity of catechol in the Kolbe-Schmitt reaction

Carboxylation of catechol could expectedly from that of mono-hydric phenolics such as phenol and guaiacol. The presence of two hydroxyl (-OH) groups in catechol creates two ortho positions, labelled as **a** and **a′** in **Scheme 5**. Additionally, carboxylation can occur at positions b and c, resulting in four possible products. The three products, 2,3-dihydroxybenzoic acid (2,3-DHBA), 3,4-dihydroxybenzoic acid (3,4-DHBA), and 2,3-dihydroxyterephthalic acid (2,3-DHTA) were commercially available and quantified using their corresponding external standards in HPLC. A significant peak was observed in the HPLC chromatogram at 22 minutes, corresponding to 4,5-dihydroxybenzene-1,3-dicarboxylic acid (4,5-DHBDC) (**Figure S5**). The combination of DOSY and COSY NMR enabled the identification of all possible products of catechol using conventional Kolbe-Schmitt reaction, which is reported here for the first time in literature (see **Figure S10 and S11**)

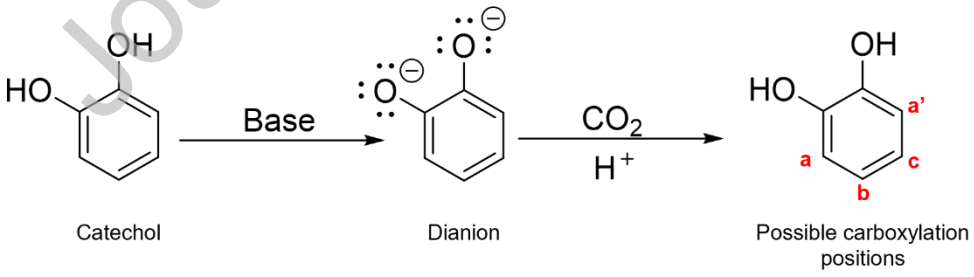

Scheme 5. Deprotonation of catechol with a base form its dianion, creating two ortho positions relative to each hydroxyl (-OH) group. Upon carboxylation, four possible positions are available for carboxylation, labelled as a, a', b, and c. Positions a and a' are symmetrical ortho positions.

The carboxylation of catechol primarily yields two major products: 2,3-dihydroxybenzoic acid (2,3-DHBA) and 2,3-dihydroxyterephthalic acid (2,3-DHTA). These products arise via the **2-HBA route**, as illustrated in **Scheme 5**, where carboxylation occurs predominantly at positions **a** and **a′**. In contrast, the two minor products, 3,4-dihydroxybenzoic acid (3,4-DHBA) and 4,5-dihydroxybenzene-1,3-dicarboxylic acid (4,5-DHBDC) are lower in yields due to steric hinderance and electronic configuration limiting this pathway [30]. Notably, simultaneous carboxylation at positions **b** and **c** is not feasible due to the resonance effects discussed earlier. Such arrangement would lead to meta-carboxylation, which is theoretically prohibited by the electronic configuration of the aromatic ring under the reaction conditions [45].

The monocarboxylic acid products, 2,3-DHBA and 3,4-DHBA, demonstrated a temperature-dependent trend (**Fig. 6**). Their yields increased from 23.16% and 3.62% at 175°C to 32.85% and 10.08% at 200°C, respectively, before decreasing to 19.79% and 9.41% at 225°C due to increased formation of dicarboxylic acid products. Although the yields were lower at 175°C, the ratio of monocarboxylation to dicarboxylation was also higher compared to 200 °C, indicating enhanced selectivity at 175°C. These trends align with literature findings, which emphasise the significance of temperature in determining carboxylation selectivity. For instance, 2,3-DHBA was reported to be favoured at 145°C, achieving a 58% yield under 56 bar CO_2 pressure after 43 hours [27]. In contrast, 2,3-DHTA was predominantly formed at 200°C, with a 56% yield requiring 90 hours under 76 bar CO_2 pressure [28].

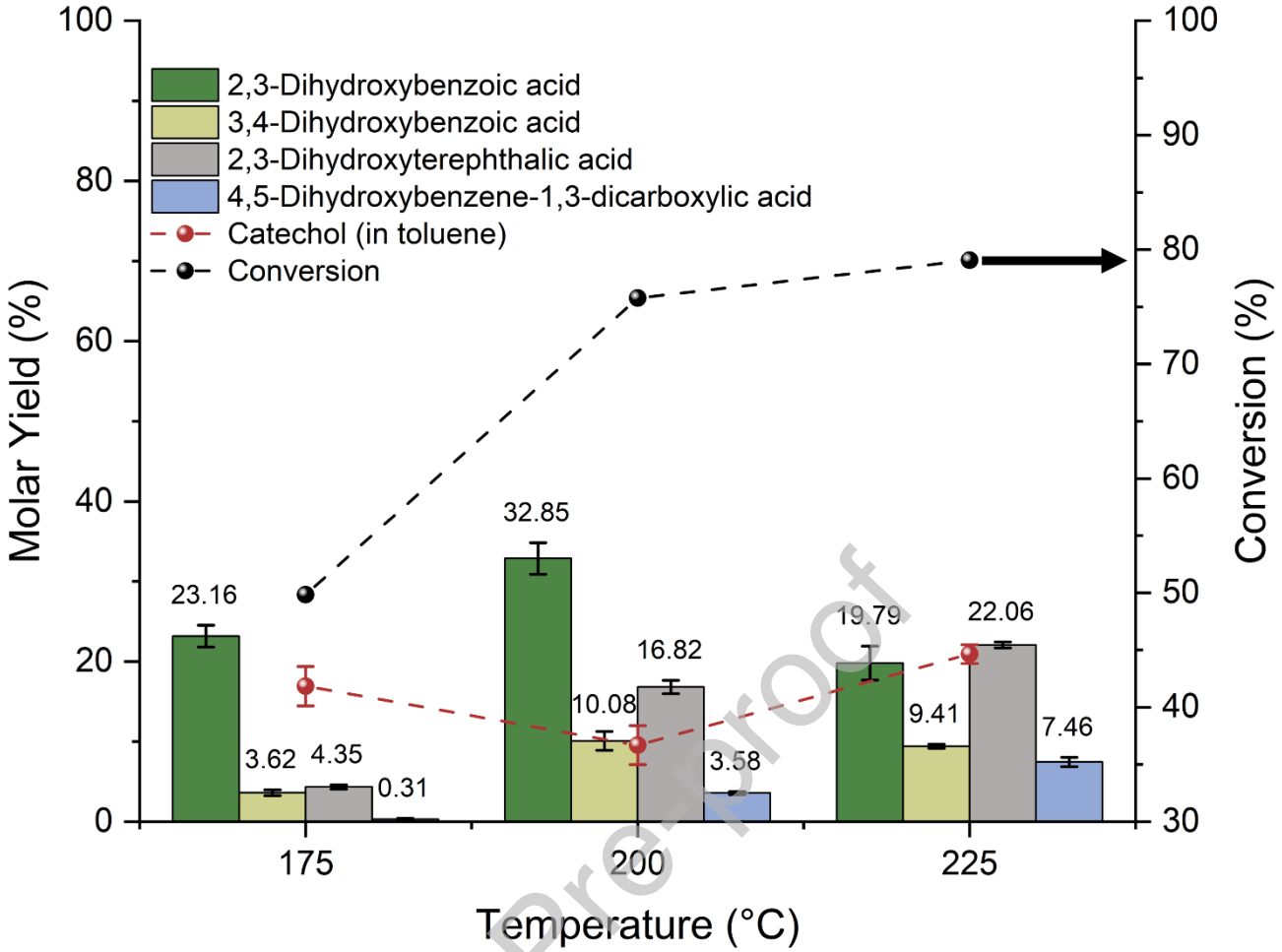

Fig. 6. Effect of temperature on product distribution and conversion of sodium catecholate in the Kolbe-Schmitt reaction. Reaction conditions: t = 2 h, sodium catecholate loading = 0.3 g, pCO_2 = 30 bar, and T = 175°C, 200 °C, and 225 °C. Error bars represent standard deviations.

For the dicarboxylic acids, the yields of 2,3-DHTA and 4,5-DHBDC increased consistently with temperature. At 175°C, their yields were 4.35% and 0.31%, respectively, increasing to 16.82% and 3.58% at 200°C, and reaching their highest yields of 22.06% and 7.46% at 225°C (**Fig. 6)**. As discussed earlier, the second carboxylation step requires higher activation energy, which is consistent with the observed temperature dependence on the product distribution with other phenolics.

The carboxylation of sodium catecholate is more complex than that of monohydric phenolics, though the reaction pathway shares key similarities. **Scheme 6** illustrates the primary mechanism (**2-HBA route**), where the reaction of sodium catecholate proceeds predominantly via pathways **S3-**

R1 and **S3-R2**. The products denoted with an asterisk (*) represent 2,3-dihydroxybenzoic acid upon acidification, while the dagger (†) marks 2,3-dihydroxyterephthalic acid.

* = 2,3-dihydroxybenzoic acid

† = 2,3-dihydroxyterephthalic acid

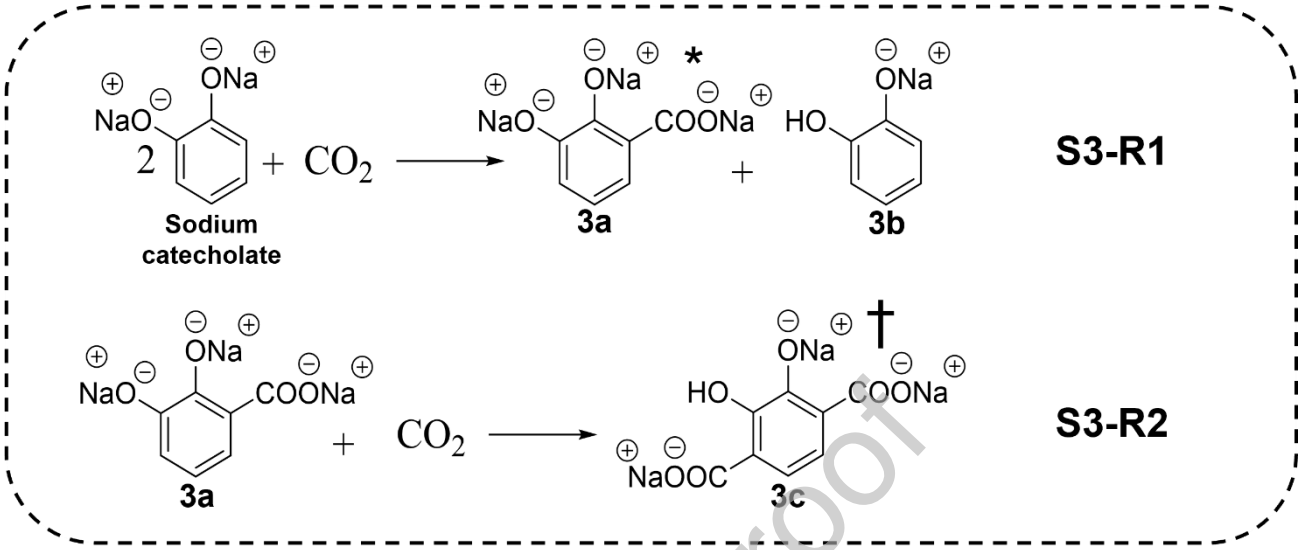

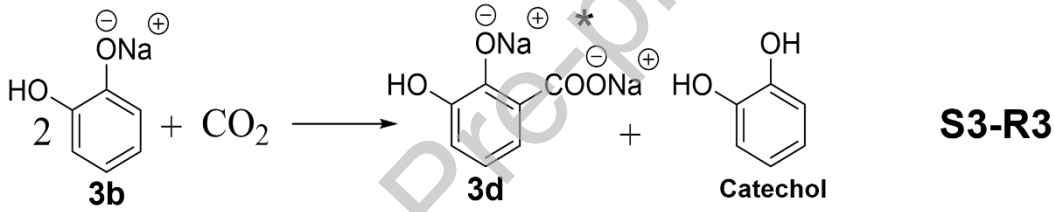

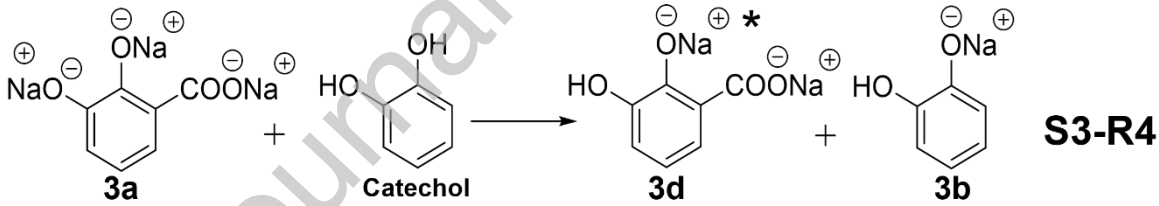

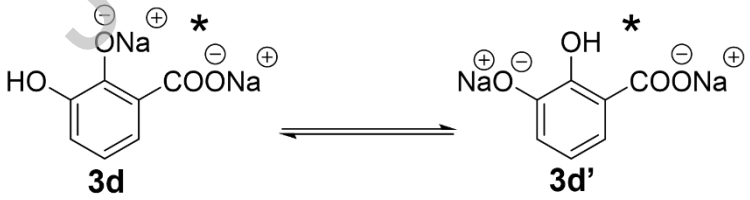

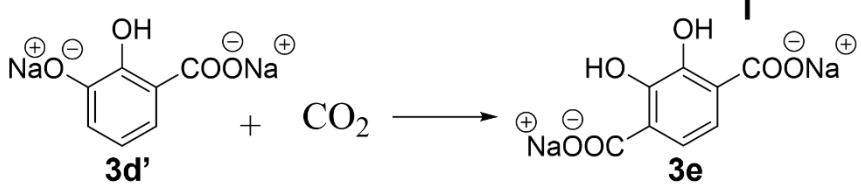

Scheme 6. Proposed carboxylation mechanism for the **2-HBA route** of sodium catecholate. The reaction proceeds via six possible pathways, labelled **S3-R1** to **S3-R6**. **S3-R5** represents the equilibrium between compound **3d** and **3d'**, as suggested in a recent report [46]. Products marked with an asterisk (*****) correspond to 2,3-dihydroxybenzoic acid, while the dagger (**†**) indicates 2,3-dihydroxyterephthalic acid upon acidification.

Initially, carboxylation occurs at **S3-R1**, yielding intermediates **3a** and **3b**. Compound **3a** has the potential to undergo further carboxylation to form compound **3c** (**S3-R2**). Concurrently, side reactions at **S3-R3** involve the reaction of two moles of **3b** with CO_2, forming one mole of **3d** and generating catechol. This behaviour is consistent with the carboxylation mechanism of monohydric phenolics [30], as compound **3b** possesses a single sodium hydroxyl group (ONa). However, compound **a** contains three sodium ions: two from the phenolic groups (ONa) and one from the carboxylation (COONa), making it highly basic and capable of acting as a Brønsted base. This increased basicity is believed to facilitate a reaction with acidic catechol, forming compounds **3b** and **3d** (**S3-R4**), imitating the second stage of the Kolbe-Schmitt reaction of phenol which was proposed earlier [30].

Recent literature suggests that an equilibrium exists with phenolate and carboxylate species [46], a behaviour also believed to take place with compound **3d**, which exists in equilibrium with **3d'** (**S3-R5**). According to Hammett's equation [41], this equilibrium introduces an electron-deficient aromatic ring, while phenoxide resonance maintains nucleophilicity at the ortho position. This increases the susceptibility for secondary CO_2 attack to yield compound **3e** (**S3-R6**). The observed reaction pattern aligns with March's mechanistic framework [45], which supports the proposed pathway. Sodium phenoxide group (-ONa) delocalises negative charge via resonance, enhancing nucleophilicity at the ortho position. Despite the electron-withdrawing effect of COONa, the resonance contribution of NaO dominates, enabling the ortho position to act as a nucleophile [30].

3.5 Temperature-dependent reactivity of syringol in the Kolbe-Schmitt reaction

The carboxylation of syringol via the Kolbe-Schmitt reaction has not been previously reported. The carboxylation of sodium syringolate into syringic acid via the Kolbe-Schmitt reaction showed very little product formation. Since the only product formation is syringic acid, the result for the carboxylation of syringic acid at various temperature has been summarised in **Table 2** below.

Table 2. Effect of temperature on product distribution and conversion of sodium syringolate in the Kolbe-Schmitt reaction. Reaction conditions: t = 2 h, sodium syringolate loading = 0.3 g, pCO_2 = 30 bar, and T = 175°C, 200°C, and 225°C.

Temperature (°C)	Compound	Molar Yield ± SD (%)	Conversion (%)
175	Syringic acid	1.53 ± 0.12	4.39
	Syringol	1.51 ± 0.10	
200	Syringic acid	0.47 ± 0.03	2.47
	Syringol	0.70 ± 0.08	
225	Syringic acid	0.52 ± 0.05	2.32
	Syringol	1.19 ± 0.07	

Note: The conversion was calculated based on unreacted syringol measured via HPLC. The absolute deviation between the total yield of products and the calculated conversion is less than ±1.33%.

The maximum yield was achieved at 175°C (1.53%), with a slight increase and no significant difference in the yield of syringic acid at 200°C and 225°C, where the yields were 0.47% and 0.52%, respectively. The carboxylation reaction of sodium syringolate is believed to proceed via the **4-HBA route**, as its two ortho positions are occupied by methoxy groups (**Scheme 7**). Although lower temperatures generally improve selectivity by favouring para-carboxylation over ortho-carboxylation, they also significantly reduce the rate of carboxylation and the overall conversion to products. In the case of syringol, however, competition between ortho and para substitution is inherently suppressed, as both ortho positions are already blocked. Therefore, temperature optimisation is mainly needed to ensure a sufficient reaction rate, rather than to control selectivity, since syringol's substitution pattern already enforces para-carboxylation. Activation effects observed when using other phenolics, as demonstrated in Section 3.6, further support this behaviour: lower temperatures did not increase the yield of syringic acid significantly, whereas higher temperatures led to significantly improved yield of syringic acid (see Section 3.6 for further discussion).

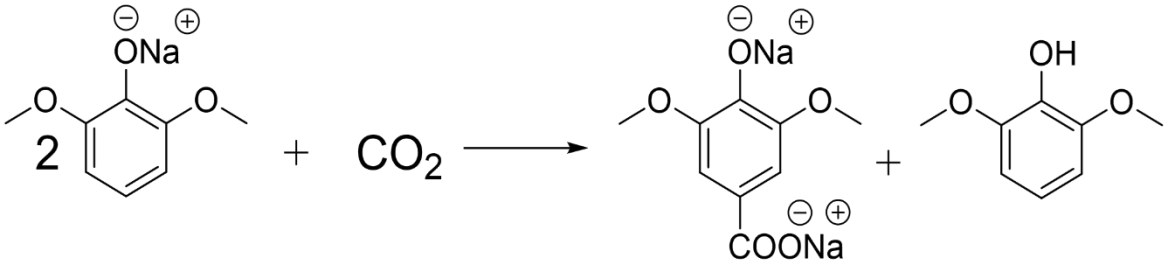

Scheme 7. Reaction scheme for the carboxylation of sodium syringolate. The reaction requires 2 moles of sodium syringolate to produce one mole of the sodium salt of syringic acid and one mole of syringol.

There has been no report of the sodium salt of syringol undergoing carboxylation via the Kolbe-Schmitt reaction, which almost exclusively favours carboxylation at the ortho position [6,47]. Syringic acid, on the other hand, is naturally found in fruits and vegetables and is primarily synthesised in plants through the shikimic acid pathway [21]. The only reported chemical route for syringic acid synthesis involves a recent patented method starting from syringaldehyde (4-hydroxy-3,5-dimethoxybenzaldehyde). The syringaldehyde-based method involves three main steps. Esterification of syringaldehyde with acetic anhydride to form syringaldehyde acetate ester (4-acetoxy-3,5-dimethoxybenzaldehyde); second, oxidation of this ester using hydrogen peroxide to yield 4-acetoxy-3,5-dimethoxybenzoic acid and finally, hydrolysis of the oxidised ester to produce syringic acid (yield = 86.5%, purity= 98.6%) [48].

3.6 Temperature-dependent carboxylation mixture of phenolics under the conventional Kolbe-Schmitt reaction

This section explores the carboxylation of a mixture of biomass-derived phenolics that can be sourced from lignin. The idea is to directly carboxylate mixtures of equimolar sodium salts of phenol, catechol, cresol, guaiacol, and syringol as the most abundant biomass-derived SPCs using the conventional Kolbe-Schmitt reaction. Importantly, this work could help to understand any synergistic behaviours of these phenolics when in mixtures.

Experiments were conducted at 175 °C, 200 °C, and 225 °C under conditions of pCO_2 = 30 bar and a reaction time of 2 hours, with 0.3 g of the phenolic salt mixture in each reactor cell. Understanding the carboxylation of phenolics derived from bio-oil could set the foundation to develop a pathway for lignin valorisation through HBAs. The carboxylation reaction products were quantified and

characterised using HPLC, with further confirmation provided by NMR analysis (see **Supplementary Materials**). **Fig. 7** presents a summary of the HBAs products obtained from the carboxylation of the phenolic salt mixtures. Each chromatographic peak showed sufficient separation and resolution for the target compounds, with retention times consistent with commercially available standards. These standards were used to generate calibration data, enabling accurate quantification of the products.

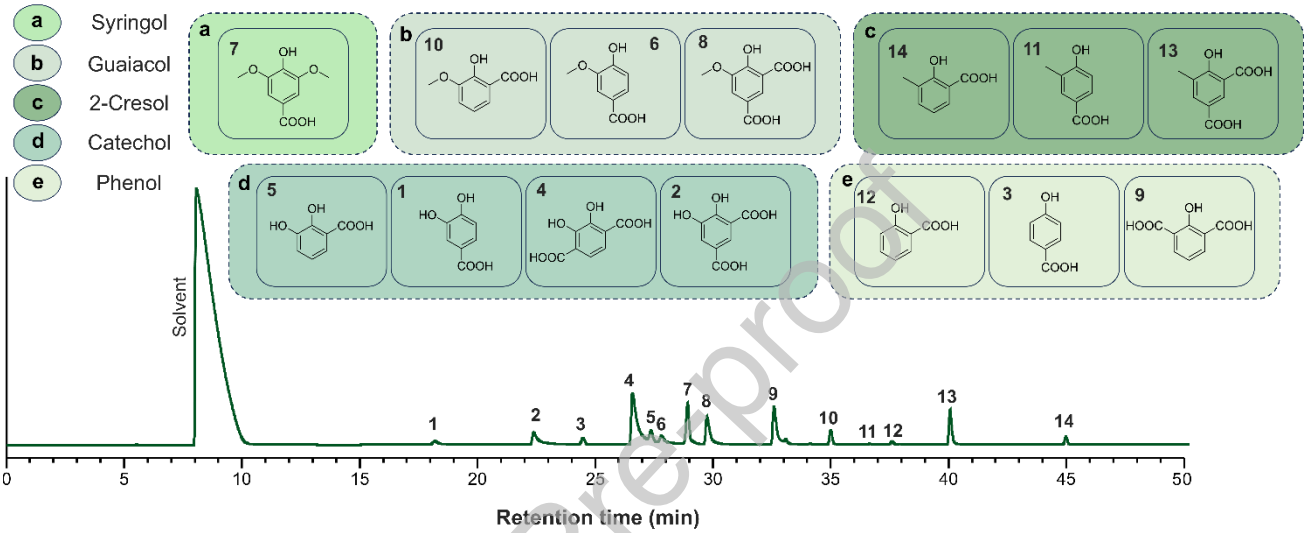

Fig. 7. HPLC chromatogram displaying the products of (a) syringol, (b) guaiacol, (c) 2-cresol, (d) catechol, and (e) phenol, along with their corresponding hydroxybenzoic acids (HBAs). Each peak is labelled with a number (1–14) corresponding to a specific HBA product.

Fig. 7 does not show any major unknown or unidentified peaks, indicating that the initial phenolic salts of the mixture (**a**, **b, c**, **d**, **e**) were successfully converted to their HBAs. However, differences are apparent in the peak intensities of the HBAs compared to the conventional products when these compounds are reacted individually. Additionally, toluene was used to recover organic compounds, and GC-MS analysis was employed as a qualitative method to detect any potential toluene-soluble organics. The results confirmed that only the aforementioned phenolics were detected as toluene-soluble organics, suggesting no formation of additional products or side reactions apart from the expected product distribution. Given that all possible products were quantifiable, the conversion percentage was calculated by dividing the total moles of products (2-HBAs, 4-HBAs, dicarboxylic acids (diacids), and phenols present in toluene) by the initial moles of phenolic salts in the reaction, and multiplying the result by 100, as shown in **Equation 5**.

$$Conversion(\%) = \frac{Total\ moles\ of\ (2-HBAs) + (4-HBAs) + diacids + phenol\ in\ tolune}{Initial\ moles\ of\ phenolic\ salt} \times 100 \quad (5)$$

Table 3 highlights the impact of temperature on the molar yields and conversions of HBAs and phenolic compounds resulting from the carboxylation of a mixture of five phenolic sodium salts. Overall, increasing the reaction temperature from 175 °C to 225 °C led to higher conversions and favoured the production of dicarboxylic acids, which are typically obtained in low yields when each salt is carboxylated individually. For instance, the sodium salts of phenol, 2-cresol, guaiacol, and catechol showed increasing yields of their corresponding dicarboxylic acids with increasing temperature, reaching molar yields of 20.5% for 2-hydroxyisophthalic acid, 14.4% for 2,4-dicarboxy-6-methylphenol, 13.6% for 2,4-dicarboxy-6-methoxyphenol, and a significant increase to 41.9% for 2,3-dihydroxyterephthalic acid. Compared to the 2-hour reaction time in this study, producing 2,3-dihydroxyterephthalic acid industrially has been reported to require 90 hours at 200°C and 76 bar to achieve a 56.0% yield [28].

In most cases, the molar yields of 2-HBAs, such as salicylic acid, 2-cresotic acid, 3-methoxysalicylic acid, and 2,3-dihydroxybenzoic acid followed a similar trend. The highest yields of 20.4%, 20.01%, 28.0%, and 15.9% for these compounds were achieved at 200°C, respectively. However, these yields declined at 225°C due to the increased formation of their corresponding dicarboxylic acids, which is consistent with the experimental trends in this study when the reactions were conducted with individual phenolic sodium salts. Furthermore, this trend supports the observation that a temperature above 200°C is required for a second carboxylation to occur. Notably, the yields of dicarboxylic acids were significantly higher in the phenolic mixture compared to individual reactions.

It could be suggested that this effect results from proton-sodium substitution among phenolic compounds formed during the first step of the Kolbe-Schmitt reaction, which depends on the acidity of each phenolic compound. For simplicity, phenol is used as an example to explain this process. As shown in **Scheme 8**, **S4-R1** and **S4-R2** represent the typical carboxylation pathways in the Kolbe-Schmitt reaction, with **S4-R2** involving phenol acting as a Brønsted acid and reacting with disodium salicylate (Na_2-SA), a Brønsted base [30]. However, in the presence of more basic compounds, such as the sodium salts of syringol and 2-cresol, phenol could preferentially undergo proton-sodium substitution with these more basic phenolic salts as shown in **S4-R3**. Such interaction could leave Na_2-SA more susceptible to further electrophilic attack by CO_2, leading to the formation of sodium 2-hydroxyisophthalate (Na-2-HIPA) via pathway **S4-R4**.

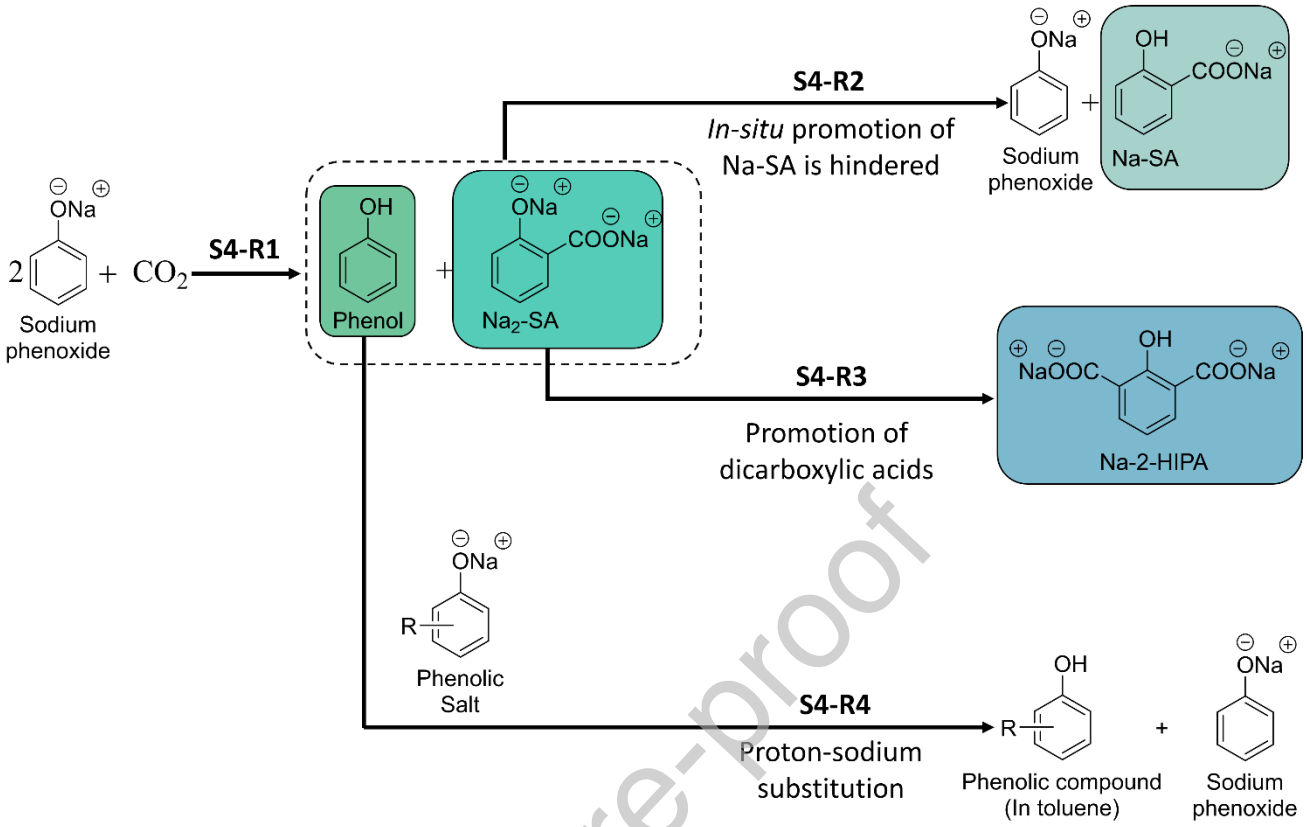

Scheme 8. Mechanistic illustration using phenol as an example in the Kolbe-Schmitt reaction within a mixture. **S4-R1** and **S4-R2** represent the typical carboxylation pathways, with **S4-R2** involving phenol acting as a Brønsted acid and reacting with disodium salicylate (Na_2-SA) as a Brønsted base. In the presence of more basic compounds, such as sodium salts of syringol and 2-cresol, phenol preferentially undergoes proton-sodium substitution with these phenolic salts (**S4-R3**). This substitution increases the susceptibility of Na_2-SA to further electrophilic attack by CO_2, leading to the formation of sodium 2-hydroxyisophthalate (Na-2-HIPA) via pathway **S4-R4**. This process results in higher yields of dicarboxylic acids during the carboxylation of phenolic mixtures.

Table 3. Molar yields of hydroxybenzoic acids (HBAs) produced from sodium salts of phenol, 2-cresol, guaiacol, catechol, and syringol in the mixture at various temperatures (175°C, 200°C, 225°C). The table also includes the molar yield of the constituent phenolics formed during the reaction and the total conversion of each phenolic salt, calculated as the sum of the yields of HBAs and their corresponding constituent phenolics.

		Molar Yield (%)			Molar yield (%)				Conversion (%)		
Na-Salts	**Hydroxybenzoic acids**	175 °C	200 °C	225 °C	Toluene Fraction	175 °C	200 °C	225° C	175°C	200°C	225°C
Sodium phenolate	Salicylic acid	22.7 ± 1.13	20.4 ± 0.62	18.6 ± 0.98	Phenol	8.59 ± 1.13	20.0 ± 2.31	20.3 ± 2.18	34.5	53.8	61.7
	4-hydroxybenzoic acid	2.76 ± 0.17	3.05 ± 0.23	2.31 ± 0.13							
	2-hydroxyisopthalic acid	0.45 ± 0.03	10.4 ± 0.16	20.5 ± 0.27							
Sodium cresolate	2-cresotic acid	16.3± 1.21	20.0 ± 1.16	12.6 ± 0.83	Cresol	10.5 ± 1.82	23.8 ± 2.11	26.0 ± 3.02	28.0	56.3	54.9
	4-hydroxy-3-methylbenzoic acid	0.24 ± 0.09	2.92 ± 0.10	1.94 ± 0.09							
	2,4-dicarboxy-6-methylphenol	1.04 ± 0.11	9.57 ± 0.72	14.4 ± 1.01							
Sodium guaiacolate	3-methoxysalicylic acid	29.6 ± 2.24	28.0 ± 2.04	15.1 ± 0.34	Guaiacol	16.2 ± 0.92	20.7 ± 1.19	22.7 ± 2.53	73.0	68.3	60.0
	Vanillic acid	19.5 ± 0.83	8.81 ± 0.14	8.60 ± 0.10							
	2,4-dicarboxy-6-methoxylphenol	7.75 ± 0.43	10.7 ± 1.10	13.6 ± 0.20							
Sodium catecholate	2,3-dihydroxybenzoic acid	15.6 ± 1.92	15.9 ± 0.98	11.8 ± 0.13	Catechol	34.6 ± 3.09	36.0 ± 1.92	25.8 ± 0.72	72.4	96.1	96.3
	2,3-dihydroxyterepthalic acid	10.5 ± 0.54	29.3 ± 1.68	41.9 ± 2.09							
	3,4-dihydroxybenzoic acid	6.61 ± 0.26	4.38 ± 0.41	4.00 ± 0.33							
	4,5-dihydroxybenzene-1,3-dicarboxylic acid	5.18 ± 1.27	10.6 ± 2.73	12.9 ± 0.30							
Sodium syringolate	Syringic Acid	4.84 ± 0.25	31.2 ± 2.30	33.0 ± 2.81	Syringol	4.63 ± 0.24	12.0 ± 0.59	17.4 ± 1.69	9.47	43.2	50.5

Consequently, higher yields of dicarboxylic acids were observed during the carboxylation of phenolic mixtures. For instance, the highest conversion and dicarboxylic acid selectivity was observed with catechol due to its high acidity, resulting from the presence of two hydroxyl groups, compared to the less acidic 2-cresol and guaiacol. The presence and position of substituents on the aromatic ring significantly influence acidity by altering the electron density around the hydroxyl group [40]. Electron-donating groups, such as the methoxy (-OCH_3) group in guaiacol and syringol, typically reduce acidity by increasing the pKa, whereas electron-withdrawing groups enhance acidity by lowering the pKa. The pKa values of these compounds are summarised in **Table S3** [49].

The formation of phenolic compounds varied significantly with temperature. For example, sodium phenoxide exhibited increasing conversion rates as the temperature increased, but phenol regeneration peaked at 200 °C (20.0%) and plateaued at 225 °C (20.3%) due to further conversion into hydroxybenzoic acids (HBAs). A similar trend is observed with the sodium salt of 2-cresol, where 2-cresol yields increased from 10.5% at 175 °C to 26.0% at 225 °C, reflecting its high conversion rates of up to 56.3%. However, for 2-cresol, higher conversion does not correspond to increased HBA yields. Although, the yield of 2,4-dicarboxy-6-methylphenol rose to 14.4% at 225 °C, the overall yield of all HBAs decreased, indicating that monocarboxylic acid products become less stable at temperatures above 200 °C, agreeing with the trends observed when the reaction was performed individually.

Similarly, the carboxylation of sodium guaiacolate showed the highest conversion at 175 °C, mainly due to the significant formation of vanillic acid (19.5%). However, at higher temperatures, the conversion slightly declined, and the yield of HBAs decreased. Instead, the yield of dicarboxylic products, such as 2,4-dicarboxy-6-methoxyphenol, increased from 7.75% at 175°C to 13.6% at 225°C. A similar behaviour was also observed with 2-cresol which is attributed to their high basicity, which promotes proton-sodium substitution reactions with more acidic phenolics like phenol and catechol, facilitating the formation of dicarboxylic acids (see **Scheme 8**).

Individually, syringol carboxylation yielded only 1.53% at 175 °C, but in a mixture, yields improved to 4.84% at the same temperature and further increased to 31.2% and 33.0% at 200°C and 225°C, respectively. Notably, the carboxylation of syringic acid via the Kolbe-Schmitt reaction has not been previously reported. Traditionally, syringic acid is produced through esterification, oxidation, and hydrolysis of syringaldehyde, achieving an 86.5 wt% yield with 98.9% purity over 20.5 hours [48]. In comparison, this method achieves a 33.0% molar yield (approximately 34.4 wt%) in a shorter time. Additionally, this process has two key advantages: it uses CO_2, a widely available and renewable carbon source, and syringol, a lignin-derived compound abundant in lignocellulosic biomass. This makes the method more sustainable and environmentally friendly for producing syringic acid.

A question may arise regarding whether the conversion of phenolics into a mixture of HBAs creates a cyclical challenge in separation. However, the industrial-scale separation of HBAs has been successfully achieved, drawing on industrial expertise and insights from the suspension-based Kolbe-Schmitt reaction [6,26–28]. Post-reaction, the phenolics formed can be separated using toluene, which retains the phenols in the toluene fraction. The remaining hydroxybenzoic acid salts can then be processed using established industrial methods. In the first step, the reaction mixture is quenched with water and subsequently acidified with HCl. This step causes the 2-HBA products to precipitate, while the 4-HBA products remain in the mother liquor [26]. A small fraction of 2-HBA, typically less than 10%, may remain in the mother liquor depending on the product distribution and the presence of substituents such as ethyl or methoxy groups [45]. Further processing involves evaporating the mother liquor, resulting in precipitated products that include some dicarboxylic acids. These dicarboxylic acids can then be separated via sublimation of the 2-HBA and 4-HBA products. This approach enables a narrower product distribution, which can either be utilised directly as a mixture or further purified for specific applications.

3.7 Effect of various phenolic compounds on sodium salt of syringol activation

The carboxylation of syringol salt presents a promising alternative production route for syringic acid. To understand the phenolics responsible for activating the syringol, the reaction was carried out by adding 50 wt% of each of the other four phenolics (phenol, 2-cresol, guaiacol and catechol) to the initial mass of the sodium salt of syringol as demonstrated in **Fig 8** (**a**). The corresponding molar yield of syringic acid resulting from addition phenol, 2-cresol, guaiacol and catechol were 16.1%, 9.31%, 23.3 and 1.58%, respectively (**Fig 8** (**b**)). The results demonstrated guaiacol as a key additive in promoting carboxylation of syringol, followed by phenol. However, in the mixture, it seems like mixture of those phenolics had a more significant synergistic effect on promotion of syringic acid as the yield were even higher at 225 °C, reaching to 33.0%. Due to increased acidity of catechol, the sodium salt of syringol acted as a carboxylating agent through substituting their sodium salt with catechol, consequently enhancing the carboxylation of catechol to selectively to produce high yield of 2,3-dihydroxybenzoic acid (72.9%). Such a novel one-pot synthesis of 2,3-dihydroxybenzoic acid has not been reported before. Indeed, it was suggested that control mechanism for production 2,3-dihydroxybenzoic acid was reported to be favoured at 145 °C, achieving a 58% yield under 56 bar CO_2 pressure after 43 hours [27]. In this present work, 14.9% higher yield was achieved with almost 20-times fold reduction in reaction time under much lower CO_2 pressure.

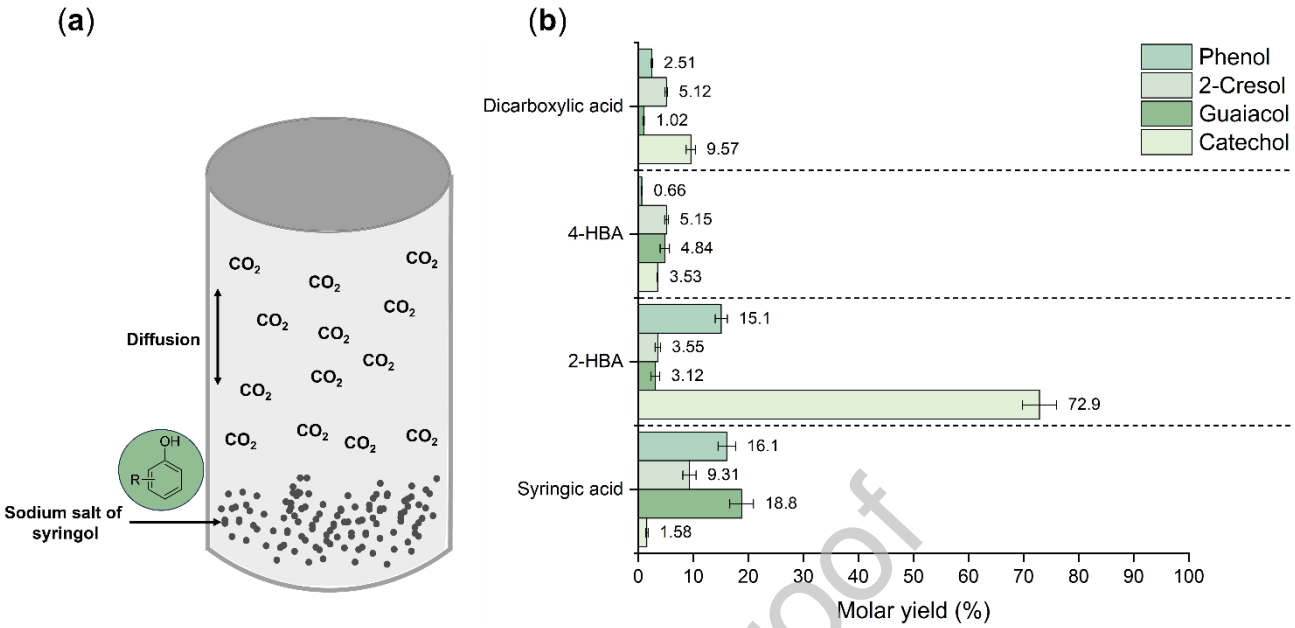

Fig 8. Carboxylation of sodium syringolate with the addition of 50 wt% phenol, 2-cresol, guaiacol, and catechol. (a) Illustration of the reaction set-up, showing sodium syringolate dispersed with the addition of the aforementioned phenolics. (b) Results of the carboxylation reaction of sodium syringolate with 50 wt% phenolic additives. Reaction conditions: t = 2 h, sodium syringolate loading = 0.3 g, phenolic additive loading = 0.15 g, pCO_2 = 30 bar, and T = 175°C, 200°C, and 225°C.

Previous research has shown recyclable additive such as 2,4,6-trimethylphenol can enhance the carboxylation of various phenolics [50], leading to increased initial carboxylation rate of various phenolics and the final yield of their corresponding HBAs. It was proposed that 2,4,6-trimethylphenol facilitates this process by absorbing CO_2 to form a reactive complex, enabling the reaction to proceed via intermolecular carboxylation of phenolics. Therefore, it would be interesting to test 2,4,6-trimethoxyphenol as recyclable additive in promotion of syringic acid. Guaiacol (single methoxy group) had the highest impact on promoting production of syringic acid. In the case of 2,4,6-trimethoxyphenol, it is anticipated it wouldn't participate in the reaction as all possible carboxylation positions are occupied with a methoxy group to produce other HBAs and selectively produce syringic acid.

4 Conclusion

Lignin-derived phenolic compounds are underutilised due to their low value, broad product distribution, and upgrading challenges caused by separation difficulties. This study focuses on upgrading these low-value phenolics - phenol, 2-cresol, guaiacol, catechol, and syringol - into hydroxybenzoic acids through direct CO_2 insertion via the Kolbe-Schmitt reaction. The selectivity of various HBAs was examined by reacting the sodium salts of the phenolic compounds individually and as their mixtures across a range of temperatures. Reactions of individual phenolics established detailed baseline reactivity, revealing temperature-dependent selectivity patterns of products not previously reported. Higher temperatures (≥200 °C) favoured 2-hydroxybenzoic acids and dicarboxylic acids, while lower temperatures promoted 4-hydroxybenzoic acid formation; however, syringol showed minimal reactivity, yielding only 1.53% at 175°C when reacted alone. This individual reactivity provided a mechanistic foundation for understanding how substituent groups and molecular structure influence carboxylation behaviour.

Building on the mechanistic insight of individual phenolics, the mixture designed to mimic phenolic-rich bio-oil, exhibited different trends with significant synergistic effects: di-carboxylation yields increased across all phenolics, particularly for catechol and phenol. Furthermore, the yield of syringic acid increased substantially in mixtures to 33.0% as temperature rose. Importantly, this study revealed synergistic effects of carboxylating phenolics in a mixture and provides better understanding into how intermolecular interactions influenced carboxylation pathways.

These mechanistic insights into temperature-dependent reactivity offer a solid foundation for extending this strategy to complex phenolic-rich bio-oils derived from lignin. This approach narrows product distributions with added-value of up to 25 times compared to unmodified phenolics, yielding HBAs and dicarboxylic acids suitable for use in polymers, pharmaceuticals, and coatings. The concept holds strong potential to advance scalable lignin valorisation and CCUS strategies, particularly for integrating CO_2-derived organic compounds into long-lived products, thereby supporting Net Zero targets.

Acknowledgements

The authors acknowledge the financial support of the College of Engineering and Physical Sciences, Aston University through the EPSRC Doctoral Training Centre, grant number EP/T518128/1 for PhD Studentship (Omar Mohammad). All technical support from the Energy and Bioproducts Research Institute (EBRI) are also gratefully acknowledged.

5 References

[1] C. Greig, S. Uden, The value of CCUS in transitions to net-zero emissions, Electr. J. 34 (2021) 107004. https://doi.org/10.1016/j.tej.2021.107004.

[2] S.T. Yang, H. Huang, A. Tay, W. Qin, L. De Guzman, E.C. San Nicolas, Extractive Fermentation for the Production of Carboxylic Acids, in: Bioprocess. Value-Added Prod. from Renew. Resour., Elsevier, 2007: pp. 421–446. https://doi.org/10.1016/B978-044452114-9/50017-7.

[3] G. Liu, S. Sun, H. Sun, Y. Zhang, J. Lv, Y. Wang, J. Zeng, Z. Yan, C. Wu, Integrated CO_2 capture and utilisation: A promising step contributing to carbon neutrality, Carbon Capture Sci. Technol. 7 (2023) 100116. https://doi.org/10.1016/j.ccst.2023.100116.

[4] W.Y. Hong, A techno-economic review on carbon capture, utilisation and storage systems for achieving a net-zero CO_2 emissions future, Carbon Capture Sci. Technol. 3 (2022) 100044. https://doi.org/10.1016/j.ccst.2022.100044.

[5] R. Schmitt, Beitrag zur Kenntniss der Kolbe'schen Salicylsäure Synthese, J. Für Prakt. Chemie 31 (1885) 397–411. https://doi.org/10.1002/prac.18850310130.

[6] A.S. Lindsey, H. Jeskey, The Kolbe-Schmitt Reaction, Chem. Rev. 57 (1957) 583–620. https://doi.org/10.1021/cr50016a001.

[7] O. Mohammad, J.A. Onwudili, Q. Yuan, A critical review of the production of hydroxyaromatic carboxylic acids as a sustainable method for chemical utilisation and fixation of CO_2, RSC Sustain. 1 (2023) 404–417. https://doi.org/10.1039/D2SU00105E.

[8] D.S. Bajwa, G. Pourhashem, A.H. Ullah, S.G. Bajwa, A concise review of current lignin production, applications, products and their environmental impact, Ind. Crops Prod. 139 (2019) 111526. https://doi.org/10.1016/j.indcrop.2019.111526.

[9] R. Shorey, A. Salaghi, P. Fatehi, T.H. Mekonnen, Valorization of lignin for advanced material applications: a review, RSC Sustain. 2 (2024) 804–831. https://doi.org/10.1039/D3SU00401E.

[10] L. Dessbesell, M. Paleologou, M. Leitch, R. Pulkki, C. (Charles) Xu, Global lignin supply

overview and kraft lignin potential as an alternative for petroleum-based polymers, Renew. Sustain. Energy Rev. 123 (2020) 109768. https://doi.org/10.1016/j.rser.2020.109768.

[11] M. Kleinert, T. Barth, Phenols from lignin, Chem. Eng. Technol. 31 (2008) 736–745. https://doi.org/10.1002/ceat.200800073.

[12] M. Singhvi, B.S. Kim, Lignin valorization using biological approach, Biotechnol. Appl. Biochem. 68 (2021) 459–468. https://doi.org/10.1002/BAB.1995.

[13] Z. Chen, C. Wan, Biological valorization strategies for converting lignin into fuels and chemicals, Renew. Sustain. Energy Rev. 73 (2017) 610–621. https://doi.org/10.1016/j.rser.2017.01.166.

[14] Z. Zhang, Q. Lu, X. Ye, W. Li, B. Hu, C. Dong, Production of phenolic-rich bio-oil from catalytic fast pyrolysis of biomass using magnetic solid base catalyst, Energy Convers. Manag. 106 (2015) 1309–1317. https://doi.org/10.1016/j.enconman.2015.10.063.

[15] V.B.F. Custodis, C. Bährle, F. Vogel, J.A. Van Bokhoven, Phenols and aromatics from fast pyrolysis of variously prepared lignins from hard- and softwoods, J. Anal. Appl. Pyrolysis 115 (2015) 214–223. https://doi.org/10.1016/j.jaap.2015.07.018.

[16] Z. Zhang, Q. Lu, X. Ye, L. Xiao, C. Dong, Y. Liu, Selective Production of Phenolic-rich Bio-oil from Catalytic Fast Pyrolysis of Biomass: Comparison of K_3PO_4, K_2HPO_4, and KH_2PO_4, BioResources 9 (2014) 4050–4062. https://doi.org/10.15376/biores.9.3.4050-4062.

[17] P. Jia, J. Wang, W. Zhang, Catalytic hydrothermal liquefaction of lignin over carbon nanotube supported metal catalysts for production of monomeric phenols, J. Energy Inst. 94 (2021) 1–10. https://doi.org/10.1016/j.joei.2020.09.014.

[18] B. Biswas, Y. Bisht, J. Kumar, S.R. Yenumala, T. Bhaskar, Effects of temperature and solvent on hydrothermal liquefaction of the corncob for production of phenolic monomers, Biomass Convers. Biorefinery (2020) 1–11. https://doi.org/10.1007/s13399-020-01012-5.

[19] Y.-J. Ding, C.-X. Zhao, Z.-C. Liu, Catalytic hydrothermal liquefaction of rice straw for production of monomers phenol over metal supported mesoporous catalyst, Bioresour. Technol. 294 (2019) 122097. https://doi.org/10.1016/j.biortech.2019.122097.

[20] A. Kazama, Y. Kohsaka, Radical polymerization of “dehydroaspirin” with the formation of a hemiacetal ester skeleton: A hint for recyclable vinyl polymers, Polym. Chem. 10 (2019) 2764–2768. https://doi.org/10.1039/c9py00474b.

[21] C. Srinivasulu, M. Ramgopal, G. Ramanjaneyulu, C.M. Anuradha, C. Suresh Kumar, Syringic

acid (SA) – A Review of Its Occurrence, Biosynthesis, Pharmacological and Industrial Importance, Biomed. Pharmacother. 108 (2018) 547–557. https://doi.org/10.1016/j.biopha.2018.09.069.

[22] S. Wang, M. Bilal, H. Hu, W. Wang, X. Zhang, 4-Hydroxybenzoic acid—a versatile platform intermediate for value-added compounds, Appl. Microbiol. Biotechnol. 102 (2018) 3561–3571. https://doi.org/10.1007/s00253-018-8815-x.

[23] Y. Song, T. Fu, J. Ning, X. Wang, J. Liu, L. Chang, Syntheses, Structure and Characterization of a New Pb(II) Coordination Polymer Based on 1,10-Phenanthroline Derivative and 5-Hydroxyisophthalic Acid, J. Clust. Sci. 35 (2024) 217–223. https://doi.org/10.1007/s10876-023-02478-9.

[24] Y. Zhou, S. Zhang, S. Huang, X. Fan, H. Su, T. Tan, De novo biosynthesis of 2-hydroxyterephthalic acid, the monomer for high-performance hydroxyl modified PBO fiber, by enzymatic Kolbe–Schmitt reaction with CO_2 fixation, Biotechnol. Biofuels Bioprod. 16 (2023) 1–12. https://doi.org/10.1186/s13068-023-02413-0.

[25] V. Kolesnichenko, G. Goloverda, R. Komati, 2-hydroxyisophthalic acid and its derivatives: methods of making and applications, WO2017222921A1, 2017. https://patents.google.com/patent/WO2017222921A1/en (accessed December 2, 2024).

[26] G. Jansen, P. Wolff, Production of sodium salicylate, 1981.

[27] J. Cason, G.O. Dyke, Preparation of 2,3-Dihydroxybenzoic Acid, J. Am. Chem. Soc. 72 (1950) 621–622. https://doi.org/10.1021/JA01157A501/ASSET/JA01157A501.FP.PNG_V03.

[28] B.C. Chen, M.S. Bednarz, J.E. Sundeen, Z.J. Zhang, T.J. Caulfield, G.S. Bisacchi, An improved large scale synthesis of 2, 3-dihydroxyterephthalic acid and dimethyl 2, 3-dihydroxyterephthlate, Org. Prep. Proced. Int. 31 (1999) 106–109. https://doi.org/10.1080/00304949909355678.

[29] T. Soderberg, Organic Chemistry with a Biological Emphasis, 2024. https://commons.libretexts.org/book/chem-106286?peerreview=show.

[30] O. Mohammad, J.A. Onwudili, Q. Yuan, R. Evans, Effective Chemical Fixation of CO_2 into Phenol Using Conventional Gas-Solid and Novel Suspension-Based Kolbe-Schmitt Reactions, ChemSusChem n/a (2025) e202402564. https://doi.org/10.1002/cssc.202402564.

[31] Biorender, Illustration, (2025). https://app.biorender.com/illustrations/66fe61ee4d665e1c4f575d6a (accessed October 10,

2024).

[32] S.E. Hashemnezhad, J.A. Onwudili, P. Thornley, K.E. Simons, Kinetics of hydrothermal reactions of n-butanol over Pt/Al2O3 catalyst for biopropane fuel gas production, Chem. Eng. J. 501 (2024) 157325. https://doi.org/10.1016/J.CEJ.2024.157325.

[33] O. Mohammad, J.A. Onwudili, Q. Yuan, R. Evans, Advancing CO_2 utilisation via suspension-based carboxylation of single and mixed biomass-derived phenolics to produce high-value hydroxybenzoic acids, Chem. Eng. J. (2025) 163498. https://doi.org/10.1016/j.cej.2025.163498.

[34] M.D. Pelta, G.A. Morris, M.J. Stchedroff, S.J. Hammond, A one-shot sequence for high-resolution diffusion-ordered spectroscopy, Magn. Reson. Chem. 40 (2002) S147–S152. https://doi.org/10.1002/mrc.1107.

[35] I. Swan, M. Reid, P.W.A. Howe, M.A. Connell, M. Nilsson, M.A. Moore, G.A. Morris, Sample convection in liquid-state NMR: Why it is always with us, and what we can do about it, J. Magn. Reson. 252 (2015) 120–129. https://doi.org/10.1016/j.jmr.2014.12.006.

[36] M. Nilsson, The DOSY Toolbox: A new tool for processing PFG NMR diffusion data, J. Magn. Reson. 200 (2009) 296–302. https://doi.org/10.1016/j.jmr.2009.07.022.

[37] A. Kojčinović, B. Likozar, M. Grilc, Sustainable CO_2 Fixation onto Bio-Based Aromatics, Sustainability 15 (2023) 16321. https://doi.org/10.3390/su152316321.

[38] K.A. Suerbaev, M.K. Aldabergenov, N.Z. Kudaibergenov, Carboxylation of hydroxyarens with metal alkyl carbonates, Green Process. Synth. 4 (2015) 91–96. https://doi.org/10.1515/GPS-2014-0098.

[39] Y. Kosugi, Y. Imaoka, F. Gotoh, M.A. Rahim, Y. Matsui, K. Sakanishi, Carboxylations of alkali metal phenoxides with carbon dioxide, Org. Biomol. Chem. 1 (2003) 817–821. https://doi.org/10.1039/b210793g.

[40] R.J. Ouellette, J.D. Rawn, Alcohols and Phenols, Princ. Org. Chem. (2015) 209–238. https://doi.org/10.1016/b978-0-12-802444-7.00008-2.

[41] L.P. Hammett, The effect of structure upon the reactions of organic compounds. temperature and solvent influences, J. Chem. Phys. 4 (1936) 613–617. https://doi.org/10.1063/1.1749914.

[42] O. Baine, G.F. Adamson, J.W. Barton, J.L. Fitch, D.R. Swayampati, H. Jeskey, A study of the kolbe-schmitt reaction. II. The carbonation of phenols, J. Org. Chem. 19 (1954) 510–514. https://doi.org/10.1021/jo01369a006.

[43] Y. Ji, Q. Yao, Y. Zhao, W. Cao, On the origin of alkali-catalyzed aromatization of phenols, Polymers (Basel). 11 (2019). https://doi.org/10.3390/polym11071119.

[44] K.A. Suerbaev, E.G. Chepaikin, N.Z. Kudaibergenov, G.Z. Zhaksylykova, Synthesis of cresotic acids by carboxylation of cresols with sodium ethyl carbonate, Pet. Chem. 56 (2016) 646–650. https://doi.org/10.1134/S0965544116070161.

[45] Smith, Michael B, Jerry March, March's Advanced Organic Chemistry reations, and Structure, John Wiley & Sons, Inc., 2006. www.wiley.com. (accessed September 19, 2024).

[46] Y. Ji, Q. Yao, Y. Zhao, W. Cao, On the Origin of Alkali-Catalyzed Aromatization of Phenols, Polymers (Basel). 11 (2019) 1119. https://doi.org/10.3390/polym11071119.

[47] H. Kolbe, Ueber Synthese der Salicylsäure, Justus Liebigs Ann. Chem. 113 (1860) 125–127. https://doi.org/10.1002/jlac.18601130120.

[48] D. Huang, Z. Yu, Synthesis method of high-purity high-yield syringic acid, CN104693022A, 2015. https://patents.google.com/patent/CN104693022A/en (accessed April 29, 2024).

[49] The Engineering ToolBox, Phenols, Alcohols and Carboxylic Acids - pKa Values, (2017). https://www.engineeringtoolbox.com/paraffinic-benzoic-hydroxy-dioic-acids-structure-pka-carboxylic-dissociation-constant-alcohol-phenol-d_1948.html?utm_source=chatgpt.com (accessed January 16, 2025).

[50] Y. Sadamitsu, A. Okumura, K. Saito, T. Yamada, Kolbe–Schmitt type reaction under ambient conditions mediated by an organic base, Chem. Commun. 55 (2019) 9837–9840. https://doi.org/10.1039/C9CC04550C.

Graphical abstract

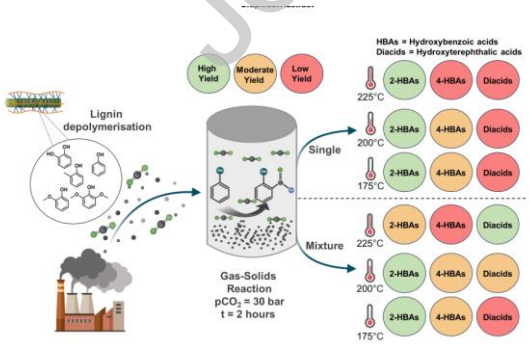

Declaration of interests

☐The authors declare that they have no known competing financial interests or personal relationships that could have appeared to influence the work reported in this paper.

☒The authors declare the following financial interests/personal relationships which may be considered as potential competing interests:

Jude Onwudili reports financial support was provided by EPSRC Centre for Doctoral Training in Technology Enhanced Chemical Synthesis. Not applicable If there are other authors, they declare that they have no known competing financial interests or personal relationships that could have appeared to influence the work reported in this paper.